An automated method for the layup of fiberglass fabric

by

Siqi Zhu

A dissertation submitted to the graduate faculty

in partial fulfillment of the requirements for the degree of

DOCTOR OF PHILOSOPHY

Major: Industrial Engineering

Program of Study Committee:
Matthew Frank, Major Professor
Vinay Dayal
John Jackman
Frank Peters
Stephen Vardeman

Iowa State University

Ames, Iowa

2015

TABLE OF CONTENTS

ACKNOWLEDGEMENTS

I would like to take this opportunity to thank my major professor, Dr. Frank who was always constructive and patient to me during my whole graduate study process. I would like to thank my committee members, Dr. Dayal, Dr. Jackman, Dr. Peters and Dr. Vardeman for their professional guidance along the way.

I would like to thank the REU (Research Experience for Undergraduates) student assistants, David, Sam, Hannah and Emily for their dedication and contribution in this research project.

I would like to thank all my colleagues in the Wind Energy Manufacturing Laboratory and the Rapid Manufacturing and Prototyping Laboratory who are always ready to help me with everything they have.

I would like to express my gratitude to my parents and family who have been encouraging me to follow my heart and pursue my dreams since I was a little boy.

ABSTRACT

This dissertation presents an automated composite fabric layup solution based on a new method to deform fiberglass fabric referred to as *shifting*. A layup system was designed and implemented using a large robotic gantry and custom end-effector for shifting. Layup tests proved that the system can deposit fabric onto two-dimensional and three-dimensional tooling surfaces accurately and repeatedly while avoiding out-of-plane deformation. A process planning method was developed to generate tool paths for the layup system based on a geometric model of the tooling surface. The approach is analogous to Computer Numerical Controlled (CNC) machining, where Numerical Control (NC) code from a Computer-Aided Design (CAD) model is generated to drive the milling machine. Layup experiments utilizing the proposed method were conducted to validate the performance. The results show that the process planning software requires minimal time or human intervention and can generate tool paths leading to accurate composite fabric layups. Fiberglass fabric samples processed with shifting deformation were observed for meso-scale deformation. Tow thinning, bending and spacing was observed and measured. Overall, shifting did not create flaws in amounts that would disqualify the method from use in industry. This suggests that shifting is a viable method for use in automated manufacturing. The work of this dissertation provides a new method for the automated layup of broad width composite fabric that is not possible with any available composite automation systems to date.

CHAPTER 1 GENERAL INTRODUCTION

1.1 Background

Composite materials, also known as composites, are materials that consist of two or more materials with different physical or chemical properties. For example, concrete is a composite material that consists of cement, aggregate and optional rebar. A wide range of materials including wood and bamboo can also be considered as composites. The material combination makes it possible to take advantage of different properties of the constituent materials. The resulting composite material can often have more favorable properties than the individual constituent materials [1]. For instance, the combination of carbon fiber and epoxy makes carbon fiber reinforced polymer (CFRP), where the carbon fiber provides the strength and the epoxy keeps the carbon fiber together. The CFRP is much stronger and stiffer than carbon fiber or epoxy alone. This work will be focused on polymer based composite, a man-made composite material that has been widely used as a manufacturing material.

Polymer based composites, also known as fiber-reinforced polymer (FRP) was introduced in the 1960s and has since then evolved to become a popular engineering material [2]. FRPs are composites made by combining reinforcing fibers in a polymer-based matrix resin [2]. FRPs are everywhere in our life today; from smaller products such as skis, bicycles and race cars, through larger products such as commercial airplanes and utility scale wind turbine blades. FRPs earned their popularity thanks to great material properties. They generally have higher strength-to-weight ratio than competing materials such as metals and plastics. In many applications they can also provide more cost effective solutions compared to the other materials. For example, most utility scale wind turbine blades nowadays are made mainly from fiberglass composites because it provides a good balance between weight, strength, stiffness and cost.

FRPs indeed have favorable properties but they are not perfect. One imperfection in using FRP is that they are difficult and expensive to fabricate. Because composites are made by combining two or more materials, their manufacturing processes can often be more complicated and problematic than for single materials. For example, many metal products can be formed by pouring liquid metal into a mold as seen in the casting process. In the similar process of forming a composite part, the reinforcing fiber has to be placed into the mold properly before “pouring” resin in by infusion. In this sense, the additional process of placing reinforcing fiber makes the composites forming process more complicated than metal forming because defects can be introduced if the reinforcing fiber is improperly placed.

1.2 Motivation

The placement of the reinforcing fiber is often referred to as the *layup* process. In this process the fiber, often in the form of dry or pre-impregnated (prepreg) composite fabrics are placed into a mold or tooling. During the layup process, the fiber has to conform to the mold without any wrinkling or waviness because wrinkles or waves can severely compromise strength and fatigue performance. Due to the difficulty and complexity of the layup process, it is most often done manually by skilled workers. In the layup process the workers place the fabric into the mold, carefully smooth it with substantial force to make it conform to the mold geometry and watch for and eliminate any wrinkles or waviness.

Figure 1 illustrates the preparation of, and layup of carbon fiber fabric for the hood of a car [3]. The fabric is cut into 2D flat patterns by a CNC cutting table, as shown in

Figure 1a. The workers then apply the fabric to the mold and use hand motion to conform the 2D fabric onto the 3D mold, as seen in

Figure 1b. This conforming or smoothing process is commonly referred to as *draping* process in the literature.

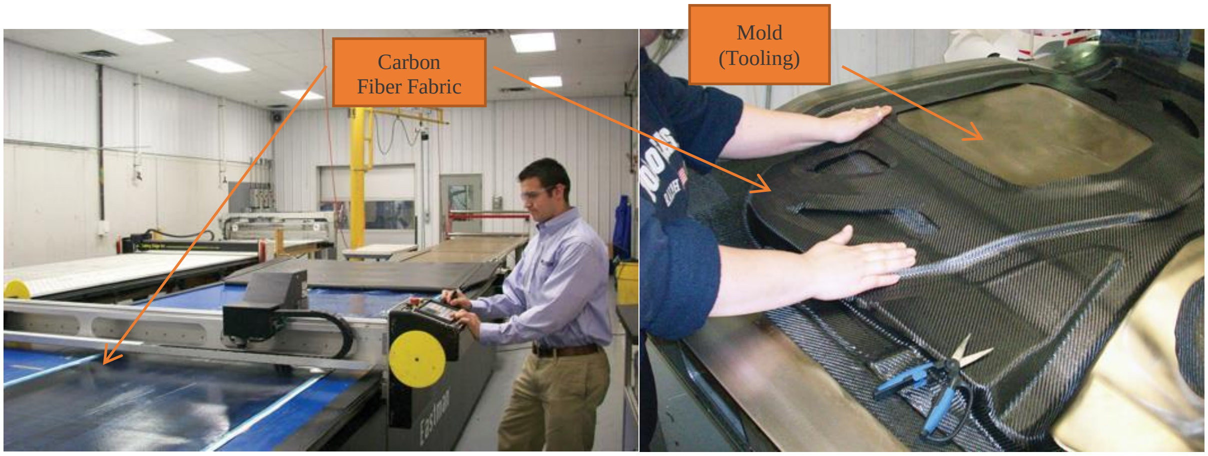

(a) (b)

Figure 1. Fabric cutting and placement, a) Cutting the carbon fiber fabric into flat pattern on a machine, and b) Laying up the flat patterns by hand onto the mold. [3]

The difficulty of the layup process is somewhat comparable to the final assembly process in automotive manufacturing. Automotive companies nowadays are able to use robots and automated machines to weld and paint car bodies but they still need workers to put electrical wiring in, secure dash boards, attach trim panels and so on [4]. Although these tasks seem repetitive and tedious, they require highly coordinated sensing, motion and judgement which is difficult or costly to obtain from robots or artificial intelligence. Similarly, when laying up fabric, workers have to use their eyes and hands to feel the fabric, use hand motion to drape the fabric, and use their judgement to determine if the fabric has been draped correctly. However, the use of skilled worker may introduce variability as human judgement can be subjective and the performance may be inconsistent. The high end composites manufacturing industry (e.g. aerospace industry) has been trying to address this issue by using automated layup technologies.

For example, Automated Tape Layup (ATL) and Automated Fiber Placement (AFP) were two such technologies developed in late 1960s and have been slowly evolving ever since.

These two technologies make use of a layup head attached to a motion system to accurately place prepreg fiber materials onto the mold. Figure 2 shows an ATL machine laying up the wing skin of a commercial aircraft [5]. However, ATL and AFP require high capital cost which prohibits them from being used in low cost applications such as the manufacturing of utility scale wind turbine blades.

Figure 2. An ATL Machine laying up the wing skin of an A350 [5].

Most of the utility scale wind turbine blades are made of composite materials and they present a somewhat unique set of challenges. First of all, wind turbine blades need to have sufficient strength and fatigue life to survive a multiple decade lifespan. Secondly, they are required to be as light as possible to maximize the power output. Moreover, the aerodynamics requires the blades to have non-prismatic geometries. Last but not least, the cost of wind blades needs to be as low as possible to make the power generated cost comparable to other sources. Composite materials are the suitable choice for wind blades because they have the flexibility to be made into three dimensional free-form shapes and they have a good balance between material properties and cost.

With the rapid growth of the wind energy industry, the size of the wind turbine blade is seeing a consistent increase to make it more cost effective [6]. Currently the common length of utility scale wind turbine blades is around 50 meters while that of the largest blades is more than 70 meters [7]. The enormous size of the wind turbine blades makes the manufacturing of them very challenging. The layup process particularly is very labor-intensive. An example is shown in Figure 3 where workers use not only hand motion but also tools like roller brushes to conform the fabric to the mold. If the fabric ply fails to be in contact with the mold, out-of-mold deformation will occur and can be considered as a defect if they are too severe.

Figure 3. Workers laying up fiberglass fabric in an LM Wind Power plant in Brazil [8].

The human interaction involved may introduce error and variability to the layup process because the variability in people's performance and subjective judgement. Additionally, the labor and training on the layup process drives up the cost of the parts. If an automated method could be used instead of human manipulation, better consistency, higher quality and lower cost of the composite parts may be achieved. Hence, an automated manufacturing technology that provides a low-cost, high-quality solution for the wind blade layup process is very desirable.

1.3 Research Problem and Objectives

Currently, there does not exist a system that has the aforementioned characteristics. The existing automated layup systems, such as ATL and AFP, work only with prepreg materials, which are not commonly used in wind turbine blades. ATL and AFP motion systems require more than six degrees of freedom, which can be costly and difficult to process plan, and typically layup material on the order of 150 to 300 millimeters wide [9]. In addition, these systems have deposition rates that are exceptionally low when compared to how much material needs to be deposited for wind blades (up to 7000 kg material to deposit for a wind blade versus several kilograms per hour [10] layup speed for an aerospace application). It would be desirable if a layup system for wind turbine blades could use a more kinematically simple method to deform the fabric to the mold and be able to handle broad width fabric panels versus narrow tapes or fibers. In previous work, Magnussen proposed a deformation methodology, referred to as *shifting* in 2011 [11] which was shown to be an effective method to make fabric follow a curved path without waviness. Although the concept was shown in prototype lab setups using simple mechanisms, a complete system was never developed. Thus the first objective of this dissertation is to create a functional shifting based automated layup mechanism. The proposed mechanism will be measured by its ability to correctly place fabric in a mold, hence the accuracy of the mechanism will be tested using industry standard materials and a relevant surrogate mold surface. Next, a process planning method for the proposed layup mechanism that can convert fabric design data into a tool path will be developed. Lastly, it remains unknown what the shifting mechanism does to the microstructure of the fabric. Material tests will need to be conducted on shifted specimens to validate that shifting can be safely used for composites manufacturing. Hence, there are three sub-objectives to accomplish.

1) **To develop an automated layup machine based on the shifting method**.

The first sub-objective is to design and implement a layup machine that makes use of the shifting deformation technique and test its ability to lay up fabric onto a desired mold surface.

2) **To develop a computer aided process planning methodology for shifting deposition**.

A process planning methodology will be developed to automatically generate desired tool paths and parameters to control the motion sequence for different mold designs with minimal human intervention, similar to the way CAM software generates NC code for CNC machining.

3) **To investigate the effect the shifting process has on fabric properties**.

The shifting technique forces fabric to change its shape by the shifting motion. The fabric's meso-scale properties will be evaluated to reveal any effect of shifting on the material.

1.4 Dissertation Organization

The work to achieve the three sub-objectives will be presented in Chapter 3, 4 and 5 as three manuscripts. Literature related to this research will be discussed in Chapter 2. The general conclusion of this dissertation and future work will be given in Chapter 6.

1.5 References

[1] Mazumdar SK. Introduction. COMPOSITES MANUFACTURING: Materials, Product, and Process Engineering2001. p. 4.
[2] Mazumdar S. Composites manufacturing: materials, product, and process engineering: CrC press; 2001.
[3] Malnati P. Corvette's carbon hood creates shock and awe. 2009.
[4] Squatriglia C. Peek Inside the Chevrolet Volt Factory. 2011.

[5] Gardiner G. A350 XWB update: Smart manufacturing. High- Performance Composites: Gardner Business Media, Inc.; 2011.
[6] Wind Power Electricity: The Bigger the Turbine, The Greener the Electricity? Environmental Science & Technology. 2012;46(9):4725-33.
[7] SIEMENS. Wind turbine with the world's largest rotor goes into operation. SIEMENS; 2012.
[8] Dantas R. LM Wind Power inaugura planta de pás eólicas. 2013.
[9] Sloan J. ATL and AFP: Defining the megatrends in composite aerostructures. High-Performance Composites: Gardner Business Media, Inc.; 2008.
[10] Domke B. Boeing 787 – lessons learnt. 2008.
[11] Magnussen CJ. A fabric deformation methodology for the automation of fiber reinforced polymer composite manufacturing. Ames: Iowa State University; 2011.

CHAPTER 2 LITERATURE REVIEW

2.1 Fabric Draping in Composites Manufacturing

Many studies have been conducted to investigate the behavior of fabrics in the draping process. Experiments have been conducted to mathematically describe the distribution and direction change of fiber tows as the fabric is draped. Computer simulation techniques were developed to predict and optimize the draping of fabrics [1-3]. In Potter and Hancock's work, drape models were used to inform the hand layup of woven fabrics. In many of the studies, a pin jointed net (PJN) model was used to model the behavior of fabric [4], which was first proposed by Weissenberg [5] from the apparel fabric industry. In this model, the tows in the fabric are assumed to be inextensible, and the joint between two cross tows was assumed to act like a pin. The tows rotate about the joint when the fabric is sheared. Shear angle is defined as the angle between warp and weft tows; which indicates the amount of shear that is applied to the fabric. The critical shear angle is reached when fabric cannot be sheared further without out-of-plane deformation, and that angle is called the shear locking limit, or the locking angle [6].

A new method called *shifting* to manipulate NCF with the purpose of creating an automated layup solution was developed in 2011[7]. In this method, a rectangular section of unidirectional fabric is sheared in the weft direction and becomes a parallelogram. By manipulating multiple successive sections, the fabric can be deformed to follow two-dimensional curves. The method has good control on shear angle and the orientation of the tows because every unit-cell in the sheared section has the same shear angle.

2.2 Automated Fabric Layup Techniques

Studies on automated fiber-reinforced polymer (FRP) layup were started in late 1960s following the introduction of Computer Numerical Control (CNC). Filament winding is one of the most commonly used automation techniques in the composites industry and has been used for decades. In this process, composite fiber is wrapped around a mandrel, as seen in Figure 4. Filament winding has a relatively high production rate and computer numerically controlled filament winding can control the placement of fibers very accurately and precisely. There have been studies on various aspects of filament winding such as tension and residual stress [8, 9]. However, this technique is limited to use for cylindrical structures such as pressure vessels and pipes [10]. The deposition rate of filament winding was reported to be up to 1360 kg/hr for simple cylindrical parts and 5 to 90 kg/hr for more complex high-performance parts [11].

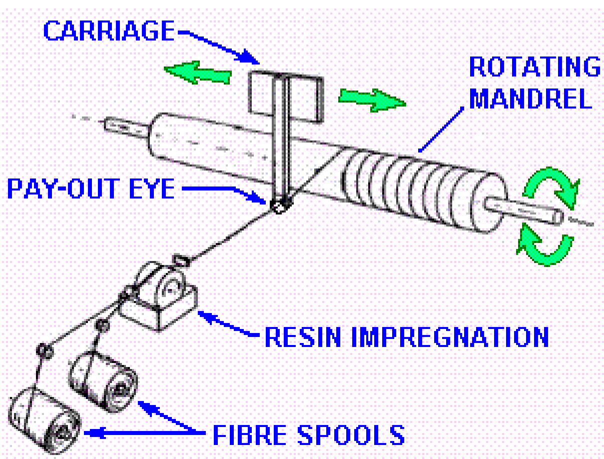

Figure 4. Schematic of Filament Winding[12].

Automated Tape Layup (ATL) and Automated Fiber Placement (AFP) are two popular automation techniques in the aerospace industry [13]. For example, the composite fuselage and wing spars of the Airbus A350XWB airplane are laid up by AFP machines, and the wing skins are laid up by ATL machines [14]. The two methods share a similar concept which is to layup preimpregnated (prepreg) fibers onto the mold surface with an end-effector mounted on the end of a robot arm or a gantry; they are both CNC-controlled. The main difference is that ATL layup uses wide prepreg tapes while AFP layup uses narrow prepreg slices sometimes referred to as *fiber tows* [15]. ATL has been widely used in creating components with large simple geometries while AFP can work on more complex geometries [16]. One such system can be seen in Figure 5 where an off-the-shelf multi-axis robot is used to carry the AFP deposition head to place carbon fiber tows onto the mold. The robotic system gives the end-effector great ability to reach designated locations of the mold, follow complex geometries and control fiber orientation. Similar to filament winding, these two techniques are numerically controlled and yield very high accuracy, repeatability and efficiency. In the manufacturing of aeronautical parts, the labor cost and the scrap rate can be significantly reduced by using ATL and AFP, although considerable investment is needed for these technologies. The investment for ATL or AFP is not cost-effective for wind blade manufacturing [17]. Moreover, the two systems mainly work on prepreg carbon fiber layup while dry E-glass layup is more common in the wind blade industry [18]. Increasing productivity and lowering the cost of the parts has been a major focus of the research on ATL and AFP [19]. The standard deposition rate for a tape lay-up head in production was reported to be 8.6 to 13 kg/h [16, 20, 21].

In addition to industrial development, many academic studies have been conducted on ATL and AFP. Lukaszewicz et al. provided a thorough summary of the publications on ATL and AFP by 2011 [15]. In the context of this dissertation, the literature on machine design, path planning and manufacturing induced defects about AFP are of the most interest. Path planning methods for AFP are summarized well by Shirinzadeh et al. in their studies on new AFP path planning methods [22].

Path planning for CNC machining has been a popular research area with many publications. Many of the principles are analogous to the path planning for the shifting machine layup. Robotics and machine vision principles are also required to guide the layup machine; methods discussed in robotics text books by Corke [23] and Craig [24] were used in the development of the layup machine.

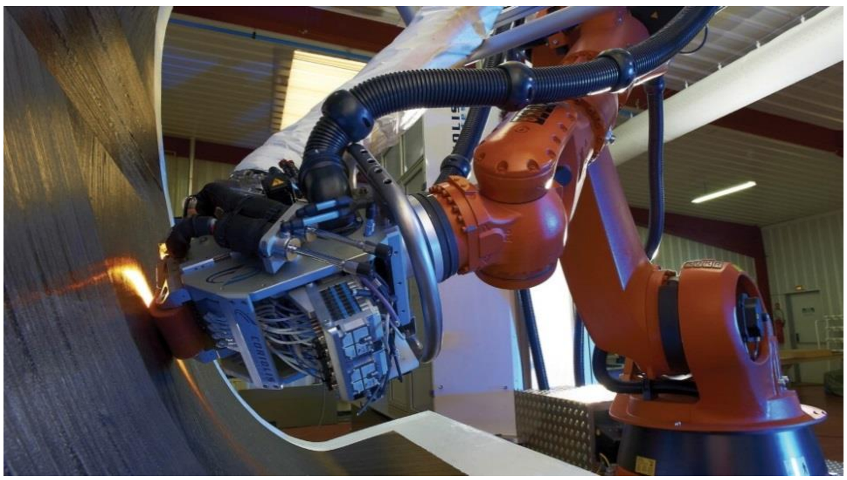

Figure 5. An AFP system that utilizes a multi-axis robot arm to place carbon fiber [25].

Vacuum forming is an automated technique to deform fabric, and is often used in fabric draping experiments. For example, Mohammed et al. [26] and Potter [27] used vacuum forming in their draping experiments. Vacuum forming can drape the fabric so that the shear angle distribution requires the least shear force. This method is not practical for large scale parts because of the scale and cost constraints.

Other automated layup methods like that of Potluri and Atkinson compared automation in the composites industry and clothing industry to find a low-cost automation solution for composites manufacturing[28]. Rudd et al. proposed a tow placement method to create a two dimensional fabric preform that has optimal tow distribution for the three-dimensional mold [29].

Various automation systems have been proposed for the manufacturing of wind turbine blades. One example is MAG's Rapid Material Placement System (RMPS)[30]. The method proposed to use a gantry system that carries a multi-axis end effector to lay up fabric on to the mold of blade shell. This system proposed a laying speed of 3m/s and application tolerance of ±5 mm. However, this system has not been seen in production to date. Crossley et al. tested ATL as a method to lay up wind energy grade prepreg E-glass on a section of a wind blade mold [31]. It was found that the difference between the E-glass and carbon fiber made the process more difficult to control. The process proved to be feasible but the production rate and the cost-effectiveness was unknown and might hinder its adoption on the shop floor.

The goal of the automation of wind turbine blade manufacturing is to reduce the cost of wind energy. Currently, the material deposition rate in wind blade industry was estimated to be 1,500 kg/h and the cost-of-finished-goods is $5/kg to $10/kg [17]. It is very challenging for the existing automated layup technologies to fulfill these requirements.

2.3 Composite Material Testing and Meso-Scale Measurement

Because FRPs are anisotropic and contain multiple different materials, the failure modes and testing methods are sometimes unique. There have been extensive studies on material test methods since the introduction of FRP in 1960s. Campbell summarized the common physical test methods for FRP composites in his book [32]. Most recently updated ASTM Composite Standards can be easily found from ASTM's website [33]. Defects can also be detected by microscopic studies on FRPs. For example, Kim et al. [34] used microscopic observation to determine fiber orientation and impregnation quality of their sheared carbon fiber tows. Raghavan [35] conducted a series of compressive strength and fatigue experiments on shifted samples in 2014, concluding that the shifting process provides suitable material properties when shifting degree is less than 10 degrees [35]. In the *extremely* shifted fabric, where tow orientation changed as much as 35 degrees, the fabric tows were found to be bent, packed and became narrower, as seen in Figure 6. The compression test data was consistent while the fatigue life data saw high variability. It remained to be seen whether packed tows potentially lowered the permeability of the fiber which may cause excessive porosity in the infused samples. Porosity in fiberglass is considered a significant defect and could reduce the fatigue life.

Figure 6. Tow bending and splitting in extremely shifted fabric.[35]

Nelson et al. conducted a series of tests on E-glass fiber glass with common defects found in wind turbine blade manufacturing [36-39]. Some of the in-plane waviness flaws identified in their tests were very similar to the ones observed by Raghavan [35].

Previous studies verified various aspects of shifting as a new manufacturing method. Magnussen conducted tensile fatigue tests with shifted samples and concluded that the more smoothly fabric is shifted (more shifts per length), the less effect it will have on material properties[40]. Raghavan conducted compressive fatigue tests and concluded that shifting had negligible effect on properties when the shift degree is less than 10 degrees [35]. The aforementioned two studies investigated the macroscopic properties of cured fiberglass with material test methods. Yet the deformation of the individual fiberglass tows during shifting was remained to be observed and understood. The dimension of the fabric at the individual tow level is also known as the *meso-scale tow structure*. Meso-scale testing in key areas of the fiberglass fabric is necessary because although the macroscopic effects are what are normally observed when a part performs, the micro- and meso-scale structures are what will cause the macroscopic effects, including possible failures [41]. Meso-scale analysis is not new to composite analysis. Composite fabric is often modeled at a meso-scale level to simulate fabric forming [42] and mechanical properties [43, 44]. Lomov et al. did a comprehensive summary on literature about meso-scale Finite Element modeling of composites [45]. Some past studies involved experiments that test the meso-scale deformation of composite fabric subjected to stress and deformation [41, 46-48]. Among them, Potluri et al. studied properties of fabric that underwent pure shearing deformation, which was very similar to shifting [49]. In that work, Potlri et al. used a flat-bed scanner to capture the tow geometry after shearing and then measured the tow widths and tow thicknesses after cutting the samples and observe the cross-sections. As shown in Figure 7, *cut 1* was along the cross tow direction, and *cut 2* was made perpendicular to the unidirectional tow direction [49]. Cut 1 was easier to make but did not expose the true tow width and required trigonometric calculations to find the true width. Cut 2, although significantly more difficult to make accurately, gave access to directly measuring the true tow width instead of being obliged to calculate it, propagating any measurement error.

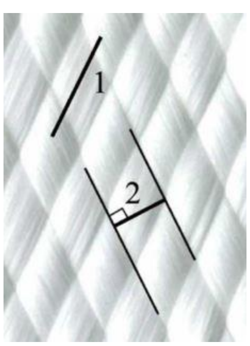

Figure 7. Sample cuts for measuring tow thickness (1) cut parallel to structural tow direction (2) cut perpendicular to unidirectional tow direction [49].

2.4 References

[1] Aono M, Breen DE, Wozny MJ. Fitting a woven-cloth model to a curved surface: mapping algorithms. Computer-Aided Design. 1994;26(4):278-92.
[2] Potluri P, Sharma S, Ramgulam R. Comprehensive drape modelling for moulding 3D textile preforms. Composites Part A: Applied Science and Manufacturing. 2001;32(10):1415-24.
[3] Van West B, Pipes R, Keefe M. A simulation of the draping of bidirectional fabrics over arbitrary surfaces. Journal of The Textile Institute. 1990;81(4):448-60.
[4] McBride TM, Chen J. Unit-cell geometry in plain-weave fabrics during shear deformations. Composites Science and Technology. 1997;57(3):345-51.
[5] Weissenberg K. The use of a trellis model in the mechanics of homogeneous materials. Journal of the Textile Institute Transactions. 1949;40(2):89-110.
[6] On the relationship between shear angle and wrinkling of textile composite preforms. Composites Part A: Applied Science and Manufacturing. 1997;28(5):491-503.
[7] Magnussen C. A fabric deformation methodology for the automation of fiber reinforced polymer composite manufacturing. Ames: ProQuest/UMI; Iowa State University, 2011.
[8] Infuluence of the filament winding tension on physical and mechanical properties of reinforced composites. Composites Part A: Applied Science and Manufacturing. 2002;33(12):1615-22.
[9] Lu H. Effects of tape tension on residual stress in thermoplastic composite filament winding. Journal of Thermoplastic Composite Materials. 2005;18(6):496-87.
[10] Design principles in filament winding. Composites Manufacturing. 1994;5(1):5-13.
[11] Strong AB. Fundamentals of composites manufacturing; materials, methods and applications, 2d ed. Dearborn: Society of Manufacturing Engineers; 2008.
[12] Filament Winding. Etamax Engineering; 2013.
[13] Tool path smoothing of a redundant machine: Application to Automated Fiber Placement. Computer-Aided Design. 2011;43(2):122-32.
[14] Gardiner G. A350 XWB update: Smart manufacturing. High- Performance Composites: Gardner Business Media, Inc.; 2011.
[15] Lukaszewicz DHJA, Ward C, Potter KD. The engineering aspects of automated prepreg layup: History, present and future. Composites Part B: Engineering. 2012;43(3):997-1009.
[16] The engineering aspects of automated prepreg layup: History, present and future. Composites Part B: Engineering. 2012;43(3):997-1009.
[17] Stephenson S. Wind blade manufacture: Opportunities and limits. Composites Technology2011.
[18] Serrano JCWJC. Composite Materials for Wind Blades. 2010.
[19] Fabrication process of open surfaces by robotic fibre placement. Robotics and Computer-Integrated Manufacturing. 2004;20(1):17-28.
[20] Advanced technology tape laying for affordable manufacturing of large composite structures. INTERNATIONAL SAMPE SYMPOSIUM AND EXHIBITION SAMPE. 1999, 2001:2484-94.
[21] Darras RS. Multiple head automated composite laminating machine for the fabrication of large barrel section components. United States of America2007.
[22] Shirinzadeh B, Cassidy G, Oetomo D, Alici G, Ang Jr MH. Trajectory generation for open-contoured structures in robotic fibre placement. Robotics and Computer-Integrated Manufacturing. 2007;23(4):380-94.
[23] Corke P. Robotics, vision and control: fundamental algorithms in MATLAB: Springer Science & Business Media; 2011.
[24] Craig JJ. Introduction to robotics: mechanics and control: Pearson Prentice Hall Upper Saddle River; 2005.

[25] Marsh G. Automating aerospace composites production with fibre placement. Reinforced Plastics. 2011;55(3):32-7.
[26] Experimental Studies and Analysis of the Draping of Woven Fabrics. Composites Part A: Applied Science and Manufacturing. 2000;31(12):1409-20.
[27] Potter K. Beyond the Pin-jointed Net: Maximising the Deformability of Aligned Continuous Fibre Reinforcements. Composites Part A: Applied Science and Manufacturing. 2002;33(5):677-86.
[28] Automated manufacture of composites: handling, measurement of properties and lay-up simulations. Composites Part A: Applied Science and Manufacturing. 2003;34(6):493-501.
[29] Tow placement studies for liquid composite moulding. Composites Part A: Applied Science and Manufacturing. 1999;30(9):1105-21.
[30] New systems automate composite wind-turbine blade fabrication, double throughput and increase quality. MAG; 2009.
[31] Automated Tape Layup (ATL) of Wind Energy Grade Prepreg Materials. 2010 European Wind Energy Conference & Exhibition2010.
[32] Campbell FC. Structural Composite Materials. Materials Park, OH, USA: A S M International; 2010.
[33] Composite Standards. 2015.
[34] Kim BC, Weaver PM, Potter K. Manufacturing characteristics of the continuous tow shearing method for manufacturing of variable angle tow composites. Composites Part A: Applied Science and Manufacturing. 2014;61(0):141-51.
[35] Raghavan LK. Industrial looks at ways of manufacturing defects of fiber reinforced polymer composites: Iowa State University; 2014.
[36] Nelson JW, Riddle TW, Cairns DS. Effects of defects in composite wind turbine blades. Round 2. Sandia National Laboratories; 2012.
[37] Riddle TW, Cairns DS, Nelson JW. Characterization of Manufacturing Defects Common to Composite Wind Turbine Blades: Flaw Characterization. AIAA SDM Conference Denver2011.
[38] Riddle TW, Cairns DS, Nelson JW. Effects of Defects Part A: Stochastic Finite Element Modeling of Wind Turbine Blades with Manufacturing Defects for Reliability Estimation. 54nd AIAA/ASME/ASCE/AHS/ASC Structures, Structural Dynamics and Materials Conference; 2013.
[39] Nelson JW, Cairns DS, Riddle TW, Workman JE. Composite Wind Turbine Blade Effects of Defects: Part B—Progressive Damage Modeling of Fiberglass/Epoxy Laminates with Manufacturing Induced Flaws. 53rd AIAA/ASME/ASCE/AHS/ASC Structures, Structural Dynamics and Materials Conference 20th AIAA/ASME/AHS Adaptive Structures Conference 14th AIAA2012.
[40] Magnussen CJ. A fabric deformation methodology for the automation of fiber reinforced polymer composite manufacturing. Ames: Iowa State University; 2011.
[41] Hamila N, Boisse P. Simulations of textile composite reinforcement draping using a new semi-discrete three node finite element. Composites Part B: Engineering. 2008;39(6):999-1010.
[42] Khan MA, Mabrouki T, Vidal-Sallé E, Boisse P. Numerical and experimental analyses of woven composite reinforcement forming using a hypoelastic behaviour. Application to the double dome benchmark. Journal of Materials Processing Technology. 2010;210(2):378-88.
[43] Edgren F, Mattsson D, Asp LE, Varna J. Formation of damage and its effects on non-crimp fabric reinforced composites loaded in tension. Composites Science and Technology. 2004;64(5):675-92.
[44] Boisse P, Gasser A, Hivet G. Analyses of fabric tensile behaviour: determination of the biaxial tension–strain surfaces and their use in forming simulations. Composites Part A: Applied Science and Manufacturing. 2001;32(10):1395-414.
[45] Lomov SV, Ivanov DS, Verpoest I, Zako M, Kurashiki T, Nakai H, et al. Meso-FE modelling of textile composites: Road map, data flow and algorithms. Composites Science and Technology. 2007;67(9):1870-91.
[46] Potluri P, Parlak I, Ramgulam R, Sagar TV. Analysis of tow deformations in textile preforms subjected to forming forces. Composites Science and Technology. 2006;66(2):297-305.
[47] Boisse P, Buet K, Gasser A, Launay J. Meso/macro-mechanical behaviour of textile reinforcements for thin composites. Composites Science and Technology. 2001;61(3):395-401.

[48] Mohammed U, Lekakou C, Dong L, Bader MG. Shear deformation and micromechanics of woven fabrics. Composites Part A: Applied Science and Manufacturing. 2000;31(4):299-308.
[49] Potluri P, Perez Ciurezu DA, Ramgulam RB. Measurement of meso-scale shear deformations for modelling textile composites. Composites Part A: Applied Science and Manufacturing. 2006;37(2):303-14.

CHAPTER 3 AUTOMATED COMPOSITE FABRIC LAYUP FOR WIND TURBINE BLADES

A paper prepared for submission to a scholarly journal

Siqi Zhu[1], Corey J. Magnussen[2], Emily L. Judd[3], Matthew C. Frank[4], Frank E. Peters[4]

The Wind Energy Manufacturing Laboratory

Department of Industrial and Manufacturing Systems Engineering,

Iowa State University, Ames, IA 50010

Abstract

This work presents an automated fabric layup solution based on a new method to deform fiberglass fabric, referred to as *shifting*, for the layup of non-crimped fabric (NCF) plies. The shifting method is intended for fabric with tows only in 0 degree (warp) and 90 degree (weft) directions, where the fabric is sequentially constrained and then rotated through a deformation angle to approximate curvature. Shifting is conducted in a 2D plane, making the process easy to control and automate, but can be applied for fabric placement in 3D models, either directly or after a ply kitting process and then manually placed. Preliminary tests have been conducted to evaluate the physical plausibility of the shifting method. Layup tests show that shifting can deposit fabric accurately and repeatedly while avoiding out-of-plane deformation.

---

[1]Primary researcher and author
[2]Second author
[3]Undergraduate research assistant
[4]Authors for correspondence

Keywords

Composite manufacturing; Automation; Lay-up (manual/automated); Wind blades; NCFs;

3.1 Introduction

Utility scale wind turbine blades are made primarily from composite materials: specifically, non-crimp fiberglass fiber reinforced polymers. With the rapid growth of the wind energy industry, the size of wind turbine blades are consistently increasing to make them more cost effective [1]. Currently, the common length of utility scale wind turbine blades is approximately 50 meters, while the largest blades are more than 70 meters long [2]. The enormous size of the wind turbine blades makes their manufacture quite challenging.

In general, the Vacuum Assisted Resin Transfer Molding (VARTM) process is widely used in the manufacture of wind turbine blades [3]. The process, which is referred to as the layup process, begins after setup with placing dry fabric into a mold. Because of the fiber flexibility, non-prismatic geometries of the mold, panel sizes, and significant amounts of fabric that need to be placed, layup is currently a very labor-intensive manual process. During the layup process, two dimensional (2D) panels of fabric are deformed manually in order to conform to the shape of the three dimensional (3D) mold. This is called draping. When placing the fabric, workers must frequently manipulate it to ensure that it is in contact with the mold or the adjacent ply. If the fabric ply isn’t in contact with the mold or the adjacent ply, out-of-plane deformation will occur and can be considered defective if it is too severe. The workers’ draping motions are very difficult to replicate with a machine because the hand movements are sensory, judgement-based, and are not necessarily the same for multiple replications. Human interaction with the layup process can introduce significant variability, causing significant scrap rates. Automated manufacturing will provide better control over the process and could yield lower scrap rates. This would result in more consistent blade construction initially and lower operating and maintenance costs over the lifetime of the blades. Additionally, automated layup would reduce the labor and training costs of the layup process.

Currently, automated tape layup (ATL) and automated fiber placement (AFP) are two automated layup techniques well-adopted in the aeronautical industry [4]. For example, the composite fuselage and wing spars of the Airbus A350XWB airplane are laid up by AFP machines, and the wing skins are laid up by ATL machines [5]. In the manufacturing of aeronautical parts, the labor cost and the scrap rate can be significantly reduced by using ATL and AFP, although considerable investment is needed for these technologies. Lukaszewicz and his co-workers provided a thorough summary of the publications on ATL and AFP by 2011 [6]. There have been studies by researchers and automation companies testing the use of ATL and AFP for wind turbine blades [7-9]. However, the investment for ATL or AFP prohibits them from being used for wind blade manufacturing [10]. Moreover, the two systems mainly work on prepreg carbon fiber layup, while dry E-glass layup is more common in the wind blade industry [11]. There are studies investigating alternative automation solutions for composite layup. For example, Tarsha Kordi et al. proposed a robotic end effector that can place fabric into a mold with a gripper and then conform the fabric to the mold with a roller [12]. Kim et al. developed a new fiber placement technique called continuous tow shearing to produce variable angle tow composites [13-15].

This paper proposes a new method called *shifting* to automate the manipulation and layup process of non-crimped fabric (NCF). The shifting method was first proposed by Magnussen in 2011 [16] as a way to manipulate fiberglass fabric without causing out-of-plane waviness. The concept of automated shifting layup is to pre-form the fabric to approximate the shape of the mold by shifting and then deposit the fabric into the mold. In this way the layup process can be completed with very little human interaction. A mathematical model has been developed to describe the method and enable process planning akin to numerical control (NC) machining code generation. A prototype machine was built to test the feasibility of an actual automated layup. The machine has performed successful layups of the trailing edge geometry of an Mega-Watt (MW) class wind blade and those results are presented.

3.2 General Solution Method

Shifting Fabric in the Weft Direction

The shifting method is intended for fiberglass NCF consisting of 0 degree (warp) tows and 90 degree (weft) tows. The act of shifting includes clamping the fabric along the fabric’s weft direction and translating the free end parallel to the clamp in order to change the direction of the fiber. This mechanism is based on the assumption of the pin-jointed net model, also known as the fishnet algorithm, which assumes the fiber to be inextensible, that the joint between the warp and weft tows to act like a pin [17], and that the tows can rotate about the jointed pin. The validity of the pin jointed net assumption has been proved by finite element analyses on the forming of both woven and non-crimp fabrics [18] and [19]. The kinematics is similar to the biaxial shear testing and the picture frame shear testing that have been used in apparel and composites tests [20-22]. As shown in Figure 8, assuming each unit cell of the fabric acts like a four-bar linkage, the whole fabric section can be deformed from a rectangle into a parallelogram. A similar approach was used by Kim et al. to achieve variable angle tows in AFP layup [13]. In the shifting method, all weft tows remain parallel to one another; therefore, fibers maintain equal lengths throughout the width of the fabric and do not form out-of-plane deformation. This process is repeated iteratively, creating a linear piecewise path. This method does, however, reduce the width of the fabric as more deformation occurs. When one wanted to have the fabric follow a curved path, it would be intuitive to “steer” the fabric through the path without applying any draping force, and waves would form as shown in Figure 9(a). Steering a roll of fabric essentially consists of rotating the axis of a roll of fabric as you deposit it into a mold. In contrast to steering, an example layup using shifting can be seen in Figure 9(b), where no waves were formed. A mathematical model is given to explain the shifting method.

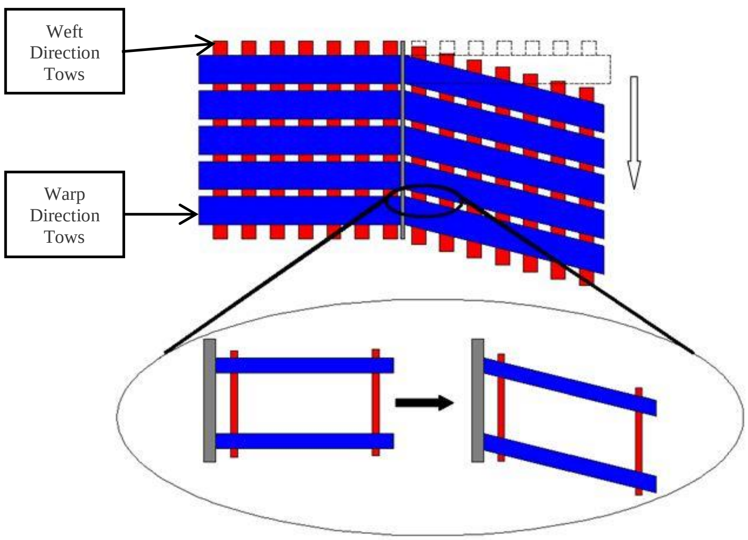

Figure 8. Shifting process on a unit section of fabric.

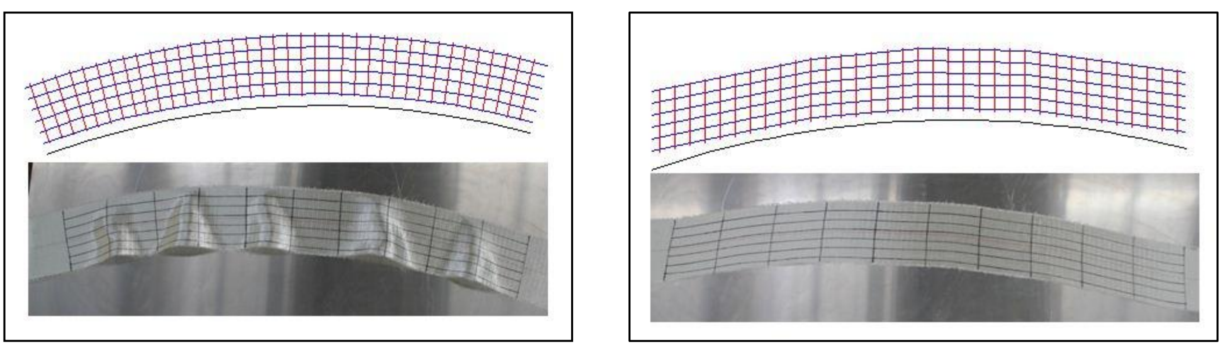

(a) (b)

Figure 9. (a) Steering - schematic and actual. (b) Shifting - schematic and actual.

Basic Mathematical Model of Shifting

To mathematically describe the shifting method, a guide curve, P(u), must first be defined. This defines the nominal center of the fabric. Next, the fabric width and placement tolerance are used to create tolerance zones (Figure 10). To create these tolerance zones, the guide curve is offset in both directions by one half of the fabric width to form the nominal edge location curves. Each nominal edge location curve is then offset in both directions by the amount of the placement variation allowed in order to form the tolerance curves. The area around each nominal edge location curve between the tolerance curves is then the acceptable region for the fabric edge, referred to here as Tolerance Zone 1 (TZ1) and Tolerance Zone 2 (TZ2).

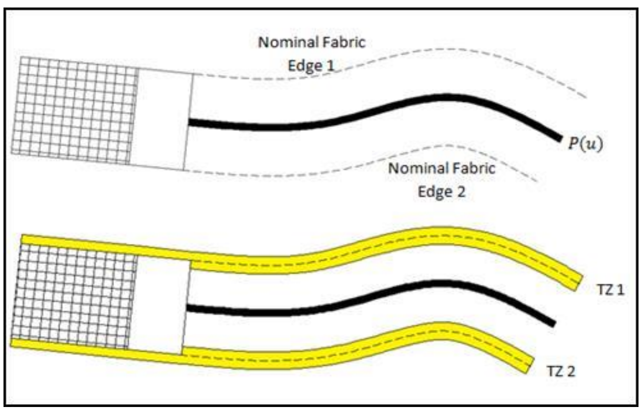

Figure 10. Guide curve and tolerance zones.

The beginning position of any tow, j, as shown in Figure 11 (a), can be calculated as:

$$T_j^0 \begin{bmatrix} x \\ y \end{bmatrix} = P(0) + [j - 0.5(M+1)]\omega_0 \begin{bmatrix} \cos(\beta + \alpha_0) \\ \sin(\beta + \alpha_0) \end{bmatrix} \quad (1)$$

where M is the number of tows in the fabric, α_0 is the nominal angle between warp and weft tows, and ω_1 is the tow spacing at α_1. For unidirectional fabrics, α_0 is 90°. All values for α_i must remain between $-\alpha_c$ and α_c, which represent the negative and positive shear lock limits.

The location of any tow j at the end of any section, i, can be represented as:

$$\mathrm{T}_j^i \begin{bmatrix} x \\ y \end{bmatrix} = \mathrm{T}_j^{i-1} \begin{bmatrix} x \\ y \end{bmatrix} + l_i \begin{bmatrix} \sin(\beta + \alpha_i) \\ \cos(\beta + \alpha_i) \end{bmatrix} \qquad (2)$$

where l_i is the length of each tow in section i, and α_i is the shear angle in section i (Figure 11 (b)).

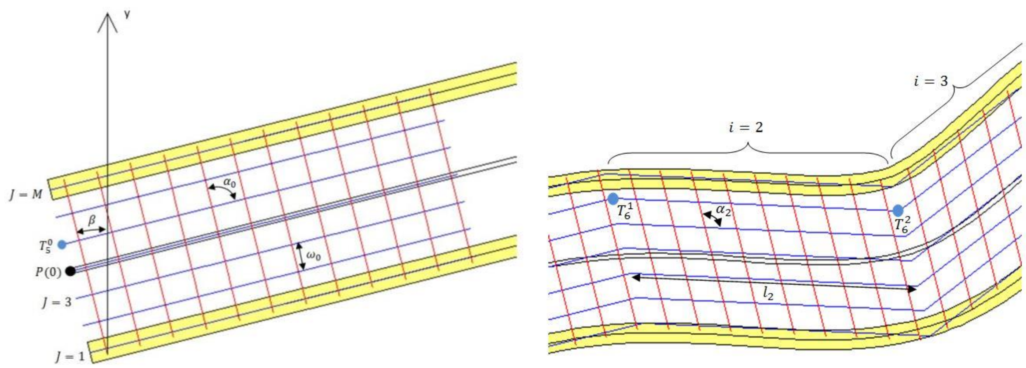

Figure 11. a) Starting position. b) Fabric variables.

To determine T_j^{i+1} from T_j^i, T_1^{i+1} and T_M^{i+1} are evaluated within TZ1 and TZ2, respectively. To do this, TZ2 is translated along $[\mathrm{T}_1^i - \mathrm{T}_M^i]$ so that T_1^i and T_M^i are at the same point. The possible locations for T_M^{i+1} include any point within the shear locking limit that is visible from T_M^i without intersecting one of the four tolerance curves. In Figure 12, α_U and α_L are the two extreme possible directions limited by the shear locking limit. The point in the tolerance zone furthest from T_M^i is then selected as T_M^{i+1}. From this, l_{i+1}, α_{i+1}, ω_{i+1}, and all other T_j^{i+1} values can be calculated.

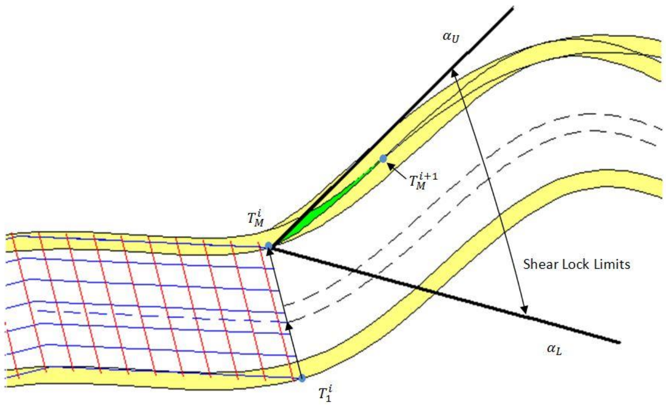

Figure 12. Path calculation for T_j^{i+1}.

Although outside the scope of this paper, the preceding model allows a point-to-point approximation of a desired path along the mold surface for layup. Analogous to NC code generation for machining, this approach would enable similar automated path planning for a shifting end-effector system. In that case, the aft end of the shifting machine represents what would be the end of a cutting tool in machining, where shift points are deposited onto the mold to approximate the desired curvature.

3.3 Implementation of the Automated Shifting Machine

Machine Design

A prototype machine test bed was developed in the laboratory on a 10×3×2 meter automated gantry system. As shown in Figure 13 (a), the machine consists of two parts: a commercially available three-axis gantry system and a prototype four-axis shifting head. The shifting head and gantry system works in coordinated motion to sequentially shift-deform and deposit the fabric onto a test mold surface. The shifting head is currently designed to shift fabric up to 280mm wide.

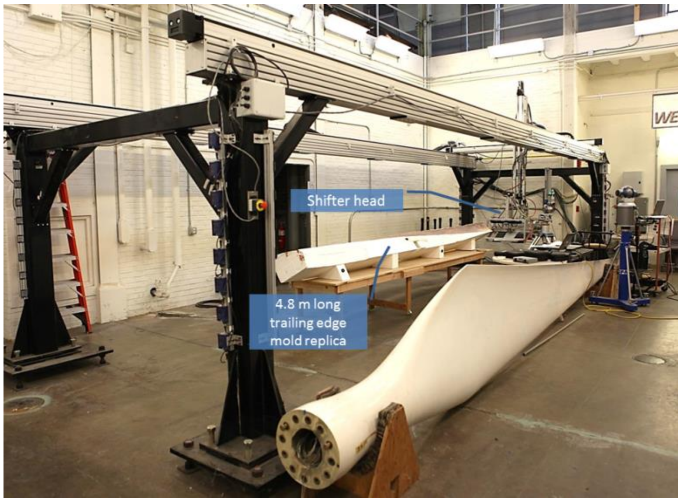

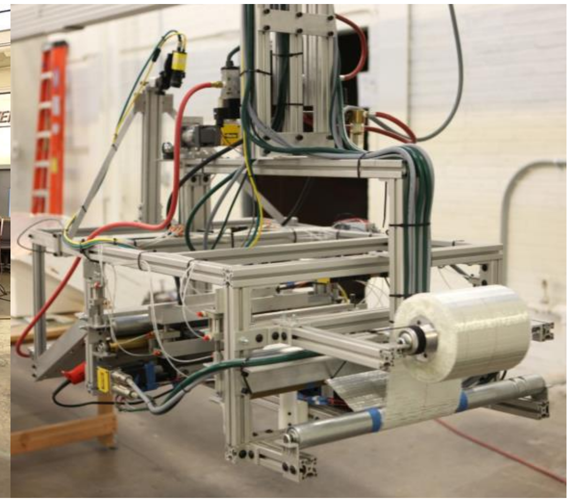

(a) (b)

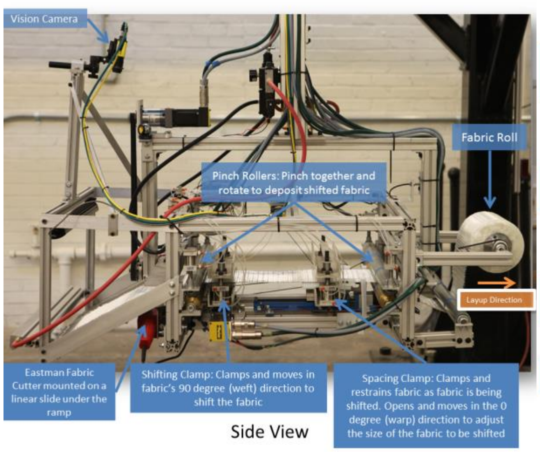

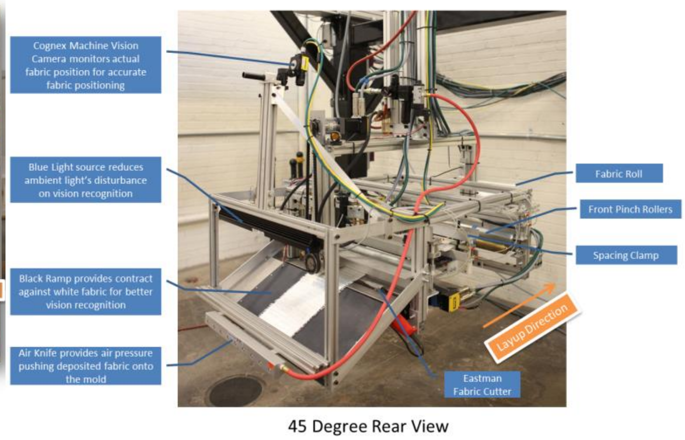

(c) (d)

Figure 13. Prototype fabric shifting machine; (a) Gantry system and shifting head, (b) front right view of the shifting head, (c) Side view, (d) rear right view.

The basic elements of the shifting head are shown in Figure 13(c). There are two clamps fixed on two linear stages to grip the fabric along the weft direction. One clamp, called the *Spacing Clamp*, moves along the warp direction of the fabric, adjusting to the length of the section to be shifted. The other clamp, called the *Shifting Clamp*, moves along the weft direction to create the shift. Two sets of pinch rollers are located outside the clamps to feed fabric from the fabric roll, which is attached to the machine. Figure 14 shows the fabric before and after a 10 degree shift.

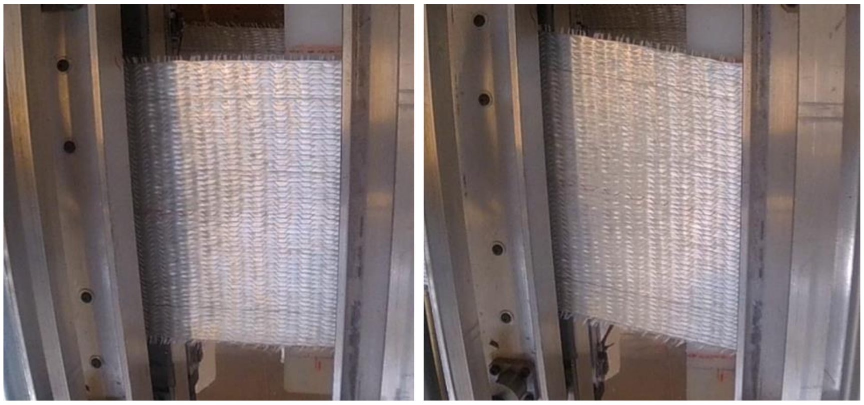

Figure 14. Fabric before (left) and after (right) shifting.

The current average deposition speed is 30 mm/s in the lab setup, limited by the capability of the gantry system (top speed = 80 mm/s, acceleration = 40 mm/s^2). Although there is limited literature on the standard human layup speed, we observed shop floor operations at a major OEM supplier, where the average hand layup speed is approximately 50 mm/s. Considering that industrial high speed gantry systems are reporting top speeds of up to 3 ~ 5 m/s with 9.8 ~ 49 m/s^2 (1 ~ 5 G) of acceleration [23, 24], the deposition speed of the machine could be increased could feasibly be increased by an order of magnitude. In addition, the lab system is designed to handle up to 280mm fabric; however, the fundamental method of shifting is not theoretically limited to any panel width. This could be a notable advantage with respect to the tapes used in current automated tape layup systems.

Work Procedure

The machine creates a shift in a cycle of coordinated motions. In each cycle, the machine feeds straight fabric from the fabric roll, shifts the fabric to a certain shape, deposits the shifted fabric onto the mold, and then prepares for the next cycle. Successive cycles of shifting result in a piece of fabric with a curved shape. The work procedure of the shifting machine is shown in the schematic of Figure 15 and explained as follows.

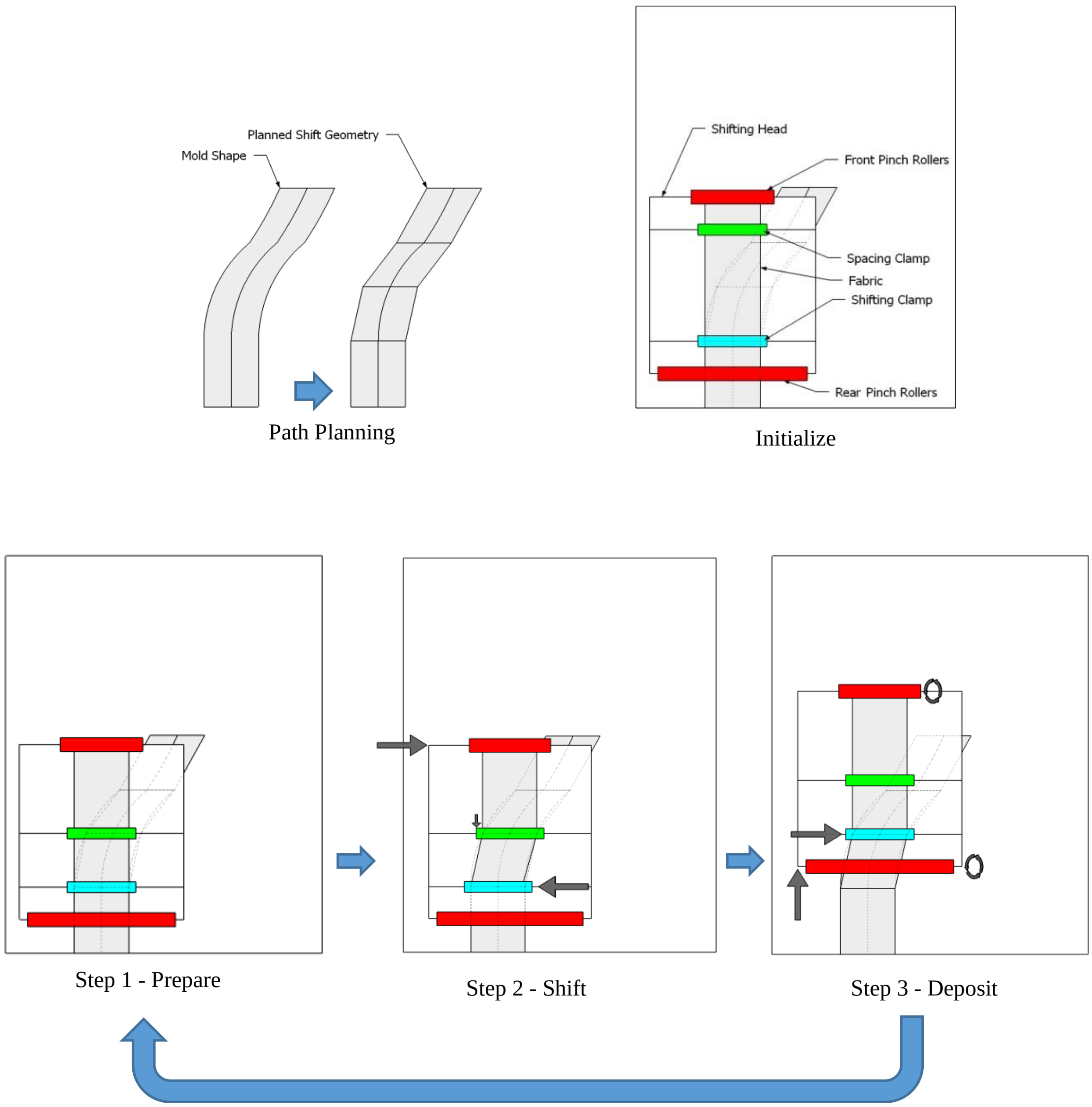

Figure 15. Working procedure of the shifting machine.

- Initialize: The shifting head moves to start position. Both rollers close and both clamps open.
- Step 1: The spacing clamp moves to the corresponding position according to the length of the shift section.

- Step 2: Both rollers open and both clamps close to grip the fabric. Next, the gantry moves the entire shifting head to position the spacing clamp while the shifting clamp synchronously moves the opposite direction to maintain position relative to the mold. At the same time, the spacing clamp moves toward the rear roller to compensate for the length reduction of the shifted fabric.
- Step 3: Both clamps open and both rollers close. Next, the entire shifting head moves forward to the next shift position as the rollers feed the fabric. The shifting clamp moves back to center synchronously. At this point, the cycle is finished and the next cycle starts from Step 1.

3.4 Experimentation

To test the performance of the shifting machine, a series of layup experiments were performed. A preliminary fatigue test was conducted to test the effect of shifting on the tensile fatigue life of fiberglass. A 2D layup test was completed to test the accuracy and repeatability of the machine. Next, a 3D layup test was completed to test the plausibility of applying the shifting technique to lay up the trailing edge prefabrication of an MW class wind turbine blade. The fabric used for the layup tests was 200mm wide Saertex 930g/m^2 unidirectional non-crimped fiberglass.

Meso-scale Deformation after Shifting

Preliminary meso-scale observation on the shifted fabric showed that most of the unidirectional tows were subjected to pure shear, while the tows adjacent to the clamps are subjected to bending (Figure 16). Tow separation in the bent section was observed when the shift angle was close to shear locking limit. The deformation was small enough to be acceptable in industrial wind blade manufacturing, where shift angle will be kept well below shear locking limit for most common used fabrics. The low level details of the meso-scale measurement analysis are outside the scope of this paper, and due to page constraints we will not present them in their entirety.

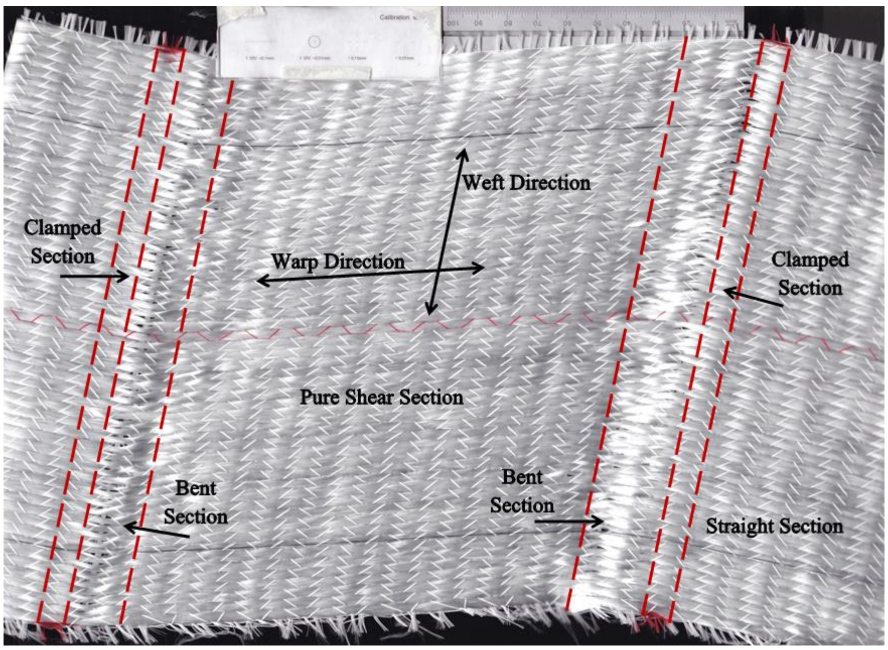

Figure 16. Meso-scale observation on the shifted fabric.

Fatigue Test

Experimental Design

A set of coupon tests were completed to test the effect of shifting on fatigue life. These coupons were comprised of 4 layers of Saertex 930 $^{g}/_{m^2}$ unidirectional fiberglass NCF cut to 25.4 mm wide and 254 mm long, vacuumed infused with Hexion EPICURE™ Resin MGS RIMR 135 and EPIKURE™ Curing Agent MGS RIMR 1366 mixed to 30 percent by weight. The tows in the coupons were kept continuous by having the coupons follow the shape of the shifted fabric as shown in Figure 17. The fabric in all coupons was shifted to approximate an arc with the same radius of 365 mm, but with different number of shifts. The coupon was divided into two, three, or four equal length sections to produce. These correspond to one, two, and three discrete shifts, respectively.

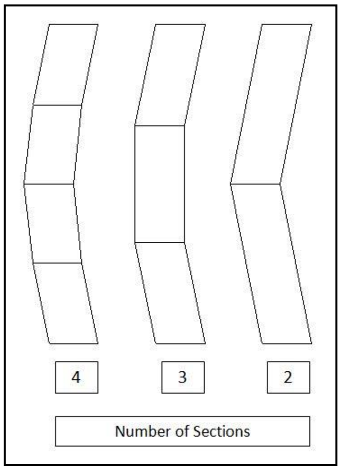

Figure 17. The shape of test coupons.

The coupons were then fatigue tested under the following condition: each cycle consisted of loading to 296MPa (43,000PSI) and relieving the coupon to 29.6MPa (4,300PSI). The frequency of testing was set at 2Hz.

Results

The fatigue life data for the nine coupons is presented in Figure 18. Life, expressed as cycles to failure, for samples with one discrete shift was very low as compared to samples with two or three discrete shifts. This shows that a large stress concentration exists at the point of the discrete shift, where all coupons with one discrete shift failed.

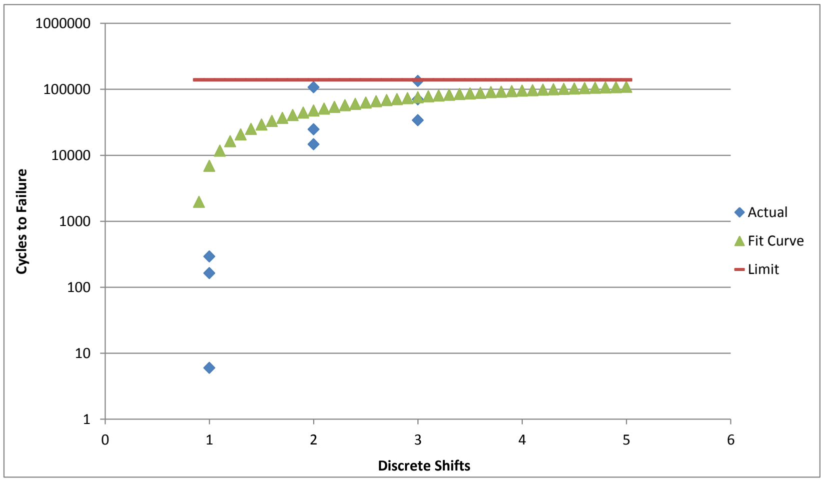

Figure 18. The effect of discrete shift quantity on fatigue life.

The life of the coupons increased very quickly as the number of discrete shifts included in the coupon increased. The fit curve for the data is in the form of:

$$Y = a - b * e^{-c*x}$$

In this equation, Y is the number of cycles and x is the number of discrete shifts. The values for a, b, and c for this angle and material are 139,424; 191,073; and 0.367, respectively, which were determined by minimizing the mean square error. In this equation, the parameter *a* represents the predicted life of a coupon with infinite shifts (continuously shifted), while *b* and *c* define the shape of the curve. The actual data along with the fit curve and limit as *x* approaches infinity.

Two-Dimensional Layup Accuracy Test

Experimental Design

In this layup test, the shifting machine was programmed to shift and lay up fabric panels onto a flat surface which is regarded as the *mold surface*. The fabric was shifted to shapes that approximate arcs with various radii. Each sample consisted of eight 200mm long sections, as shown in Figure 19(a). Sections 1~6 were shifted sections that approximated an arc with a certain radius, while sections 0 and 7 were non-shifted portions on the two ends.

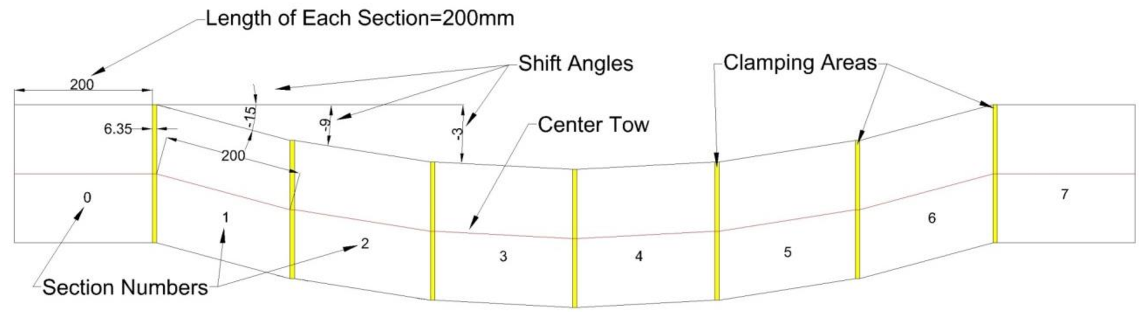

(a)

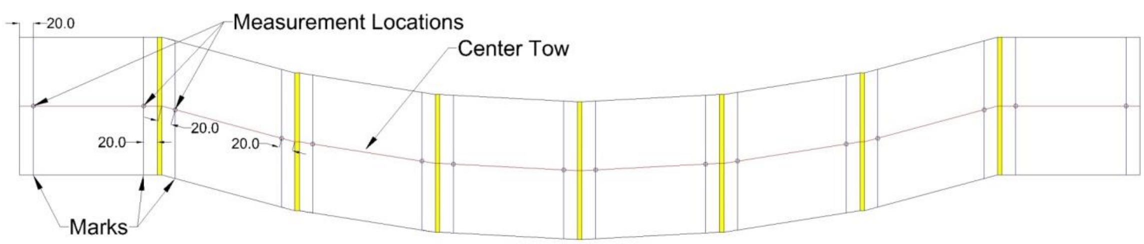

(b)

Figure 19. Two-dimensional sample layout: (a) Planned geometry of a sample with radius of 2.0 m. (b) Measurement locations of a sample with radius of 2.0 m.

As discussed in the Methods section, the direction of the unidirectional tows changes when fabric is shifted. The angle between the unidirectional tows before and after the shifting is called the “shift angle.” In the layup samples, each section was shifted to a certain shift angle by the machine, which is called the *prescribed* shift angle; for the non-shifted sections, the shift angle is considered to be zero. The prescribed position of the fabric can be calculated using the prescribed angle. After the fabric was deposited onto the mold, the actual position of the manipulated fabric was measured and compared to the prescribed position. When shifted, all of the unidirectional tows were kept parallel to each other and had the same geometric profiles. Thus, the profile of one of the tows can be used to approximate the shape and position of the entire section of the fabric sample. In these experiments, the position of the center tow of fabric was measured using an articulated Coordinate Measurement Machine (CMM), the Faro EDGE Arm. Figure 19(b) shows the measurement locations of the fabric. For each shifted section, two points close to the shift location were measured.

A metal square was fixed at the corner of the mold surface to construct a coordinate system for the Faro Arm, as shown in Figure 20. A metric scale was positioned beneath the plastic mold surface in order to locate the probe of the Faro Arm during experiments. A reference sphere on the corner of the shifting head was scanned with the Faro Arm for each trial to ensure that the machine started in the same location. In this way, measurement of the layup process of all the samples was performed using the same global coordinate system.

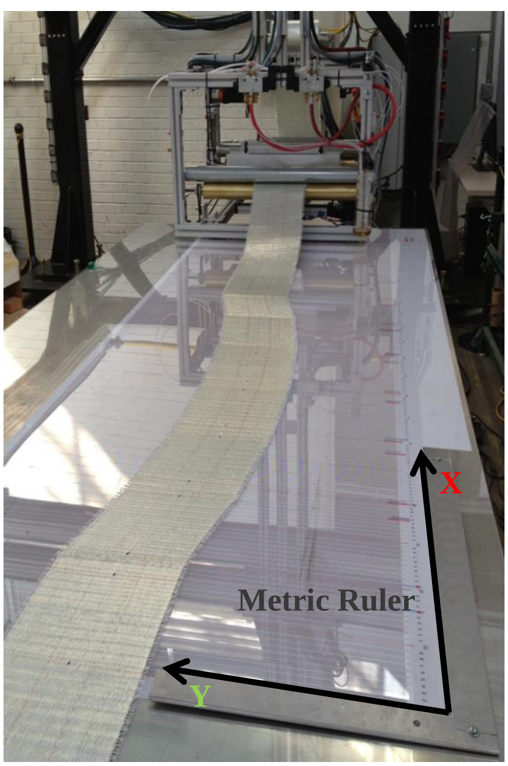

Figure 20. The measurement coordinate system.

To understand the influence of different variables, two layup experiments were conducted. In the first experiment, samples with four different radii were created to investigate if the layup performance varies for different geometries. In the second experiment, a technique called *Over Shifting* was developed and tested to see if it can improve the locational accuracy of the samples. Table 1 presents the experiment plan.

Table 1. Experiment plan for two-dimensional layup test.

Experiment a) Effect of Geometry										
Group #	Radius (mm)	Shift Angles (degree)						Length of Each Section (mm)	Replications	Variable
1	6099	5	3	1	-1	-3	-5	200	5	Radius
2	3050	10	6	2	-2	-6	-10			
3	2033	15	9	3	-3	-9	-15			
4	1525	20	12	4	-4	-12	-20			
Experiment b) Effect of Over-Shifting										
Group #	Radius (mm)	Shift Angles (degree)						Length of Each Section (mm)	Replications	Variable
3	2033	15	9	3	-3	-9	-15	200	5	No Over-Shift
6										30% Over-Shift
7										50% Over-Shift

Results

a) Effect of Different Geometries

It was observed during preliminary tests that when the fabric was shifted, the actual shape was usually different compared to how it was theoretically shifted. The goal of this experiment was to understand if different prescribed geometries (varying radii) affect the final sample geometry or variability. The machine was programmed to create fabric samples with four different radii, with five replications for each. The length of each section was 200mm. By adjusting the shift angles from 1 to 20 degrees, the radii varied from 1.9m to 6.1m. Since this type of fabric is estimated to have a shear locking limit of 25 degrees, this experiment tested most of the shift angles that could reasonably be induced to the fabric under typical use. The sequence of experiments was randomized prior to execution. Figure 21 indicates the actual positions of the shifted fabric compared to the prescribed (programmed) position. Since the X-coordinate locations of each measuring point were the same, the actual position of the fabric could be analyzed by the Y-coordinate location of the measured points. As shown, actual positions of the fabric tended to locate greater than prescribed positions for the first half of sections and lower than prescribed positions for the second half of sections. This phenomenon can be explained by the fabric's natural tendency to spring back elastically.

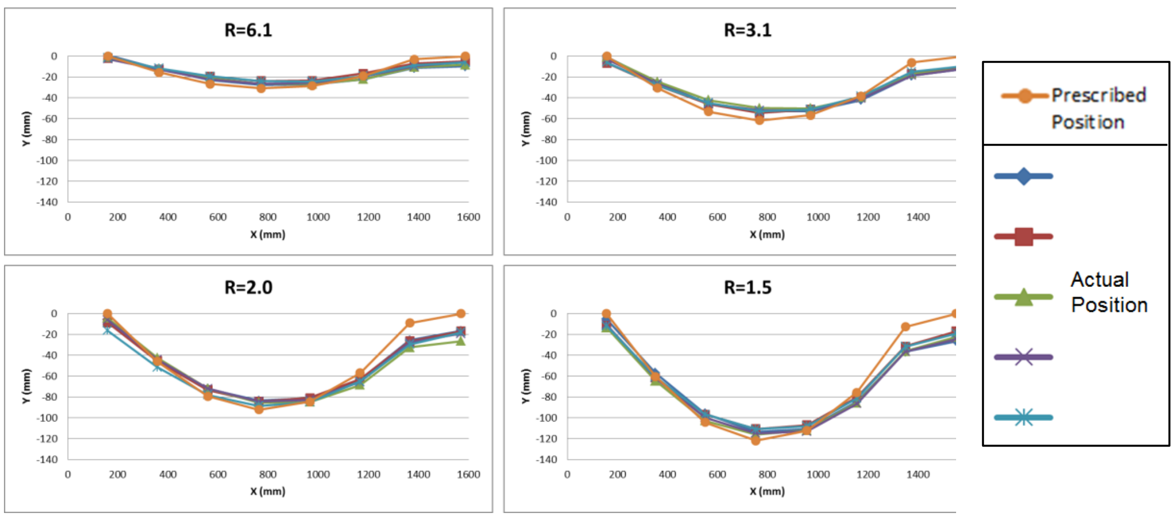

Figure 21. Prescribed and actual position of the shifted fabric in a 2D coordinate system.

Figure 22 presents the average positional deviation at each section and for each radius. The samples with tighter curvature generally have more deviation, and the last two sections have larger deviation than the other sections. In addition, more of the sections are biased clockwise toward the negative Y direction. The error bars provide the variability of the fabric positions as the width of the 95% confidence interval of Y position. Most of the interval is within 10mm, indicating that the machine is precise enough to place fabric within 10 mm around the mean location. Notably, the largest variability occurred in the samples with smaller radii.

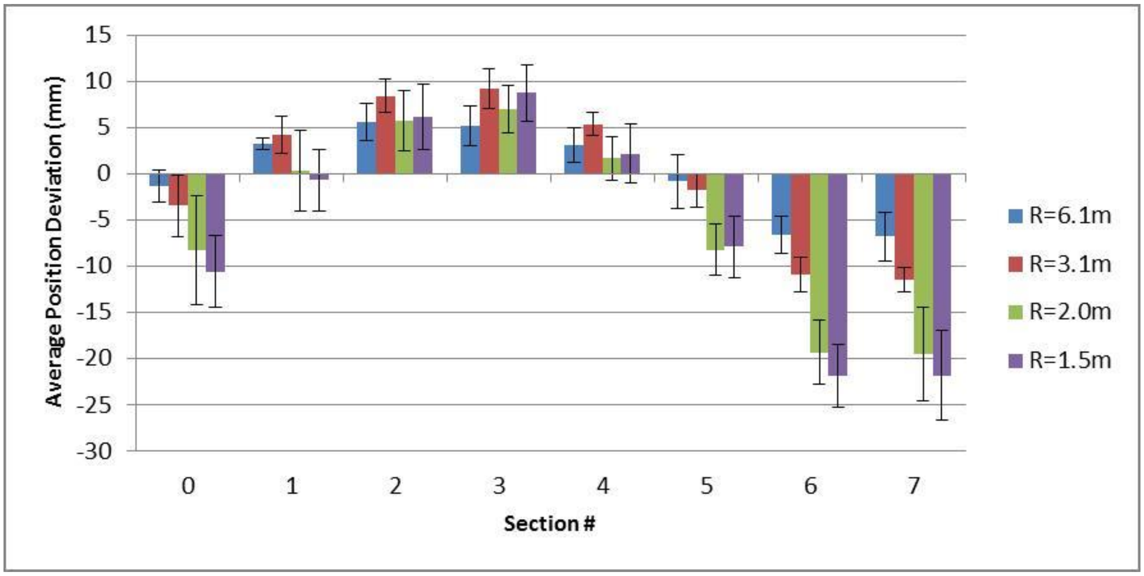

Figure 22. Average position deviation of each section and radius.

b) Effect of Over-Shifting

In the preliminary tests, the actual shift angle was usually smaller than the prescribed shift angle. It was hypothesized that the fabric pulled the shifted section back towards its original shape in a form of *spring back* or recovery. This phenomenon has been observed by previous studies on fabric shearing properties but has not been thoroughly discussed [20, 25]. Through a proposed method of *over-shifting*, the fabric is shifted to a larger angle at first, and then it is shifted back to the prescribed angle. The amount of over-shift is defined as the percent to which the fabric is shifted before it is shifted back to the final shift angle. For example, if a section is planned to be shifted to 10 degrees, a 50% over-shift means it is first shifted to 15 degrees and then shifted back to 10 degrees. Two different percentages of over-shifting were tested by creating samples with the same 2033mm radius, as shown in Table 1.

The results in Figure 23 and Figure 24 show that the positional deviation of the over-shifted samples is significantly smaller than that of the non-over-shifted samples at several sections. Additionally, the over-shifted samples have lower variability in every section, which indicates that over-shifting could make the layup process more repeatable. In addition, a Fisher's Least Significant Difference Test confirmed that the over-shifted samples have lower deviation for the latter three sections 5, 6 and 7. The deviation of the over- shifted samples is within ±10mm, while the deviation of the non-over-shifted samples is as large as ±25mm.

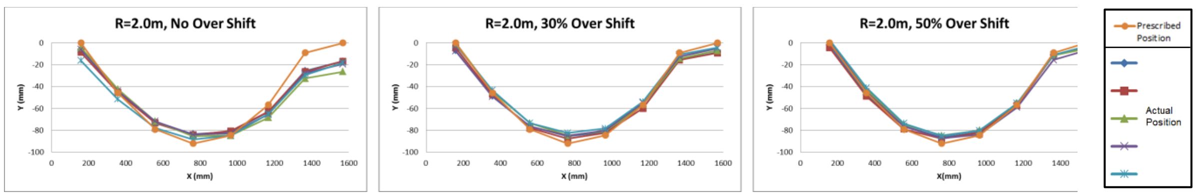

Figure 23. Effect of over-shifting.

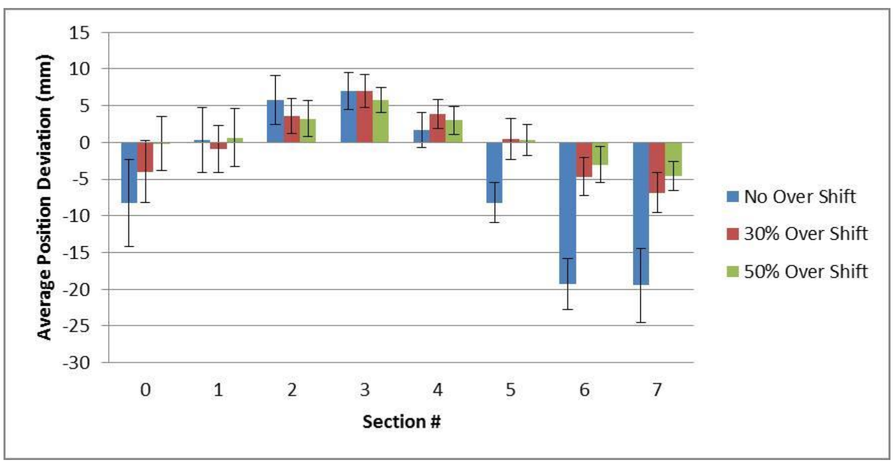

Figure 24. Average positional deviation for over-shifted versus non over-shifted samples.

Three-Dimensional Layup

As a more practical and applied evaluation, the machine was used to lay up the trailing edge prefabrication for an MW class wind turbine blade. As seen in Figure 25, the mold design includes the geometry change along the trailing edge from horizontal to near vertical, which requires substantial fabric shearing during the layup process. On the shop floor, workers must apply intensive hand manipulation in order to smoothly drape the fabric to avoid any waviness. Although shifting is conducted in a 2D plane, the end-effector system enables the shifting head to deposit the shifted fabric onto a 3D surface through the use of a roll axis. A 3D layup test was performed to test the repeatability of the system, where twelve iterations of a 4 meter long sample were deposited onto the mold. The position of the fabric relative to the mold was measured for each sample using a Faro Arm. To evaluate the sample, five reference locations uniformly distributed along the samples were marked on the mold. From each reference location, a line was scribed perpendicularly across the mold. After a ply of fabric was deposited, the intersecting points between the fabric's edge and each of the five scribed lines were measured using the Faro Arm (Figure 26). By comparing the results of the twelve iterations, the repeatability of the positioning of the fabric could be estimated. The result of these tests is presented in Table 2.

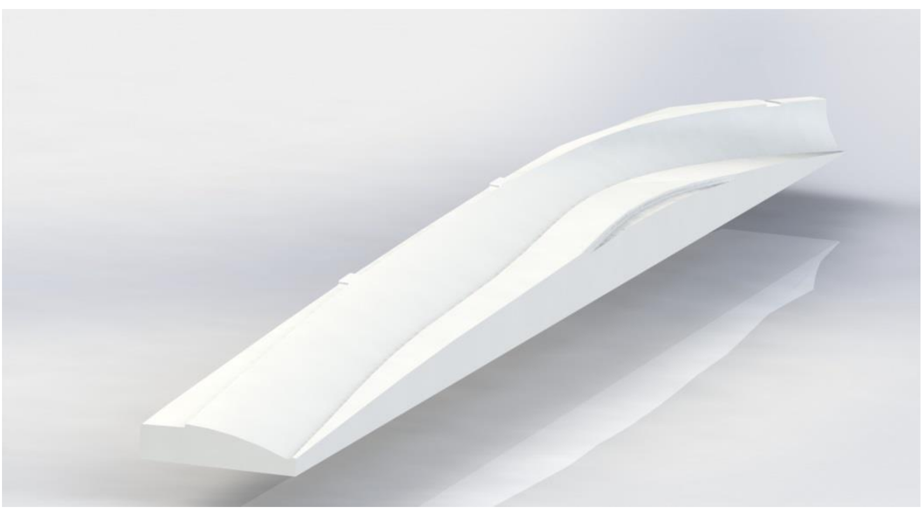

Figure 25. CAD model of trailing edge prefabrication mold.

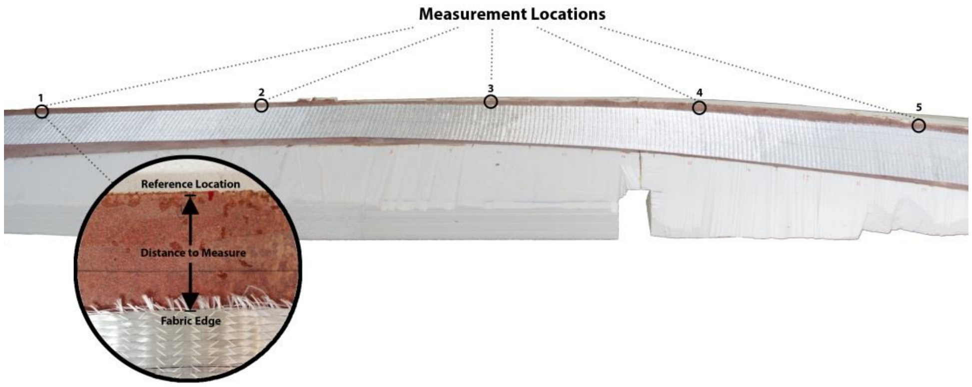

Figure 26. Measurement of fabric position along the mold.

The results show that the positional variation is generally lower at the beginning and increase significantly for the latter two positions, where the mold surface tends more toward vertical orientation. It is assumed that when the fabric is laid on more vertical sections, simple gravity pulls the fabric, affecting the actual shift angle and position, especially since no tackifier adhesive was applied in this test. Future additions to the shifting head can easily include a simple tackifier spraying beneath the aft ramp where the fabric drops onto the mold. The current system uses an Exair air knife to apply non-contact pressure on the fabric to reduce this issue. Regardless of these initial challenges, the system notably applied the fabric panels without waviness. Considering the skilled workers' required complex manipulations observed in the factory, the fact that the automated system applied smooth panels onto a 3D surface is a notable accomplishment. The positional results are arguably quite promising: the standard deviation of the fabric panel position was close to 1mm on average across sections, which gives a 95% prediction interval of ±2 mm. This level of quality would be difficult to achieve today using hand layup of fabric in the plant, and future refinements of the shifting apparatus could provide much better accuracy and precision.

Table 2. Results of repeatability testing on trailing edge mold.

Location / Iteration	1	2	3	4	5
1	58.30	36.40	23.72	32.94	23.46
2	57.15	35.24	24.42	32.56	25.62
3	56.81	36.38	25.64	35.25	26.68
4	56.79	35.85	25.11	32.07	23.70
5	57.23	35.57	24.40	29.67	22.31
6	56.76	35.67	23.84	30.62	24.11
7	56.93	36.55	24.09	32.99	24.44
8	58.12	36.94	24.47	32.49	26.06
9	57.15	34.06	24.29	31.79	24.90
10	58.19	35.80	23.69	35.07	25.38
11	57.12	35.58	25.02	32.64	26.68
12	56.15	36.12	24.67	31.92	23.62
Range	2.15	2.88	1.95	5.58	4.37
Standard Dev	0.66	0.74	0.59	1.57	1.38
95% Prediction Interval	μ±1.31	μ±1.49	μ± 1.19	μ±3.14	μ±2.75

Unit: mm

3.5 Conclusions

The proposed fabric shifting method has been generally shown to be a feasible method to manipulate fiberglass fabric automatically, with a relatively simple kinematic system. Initial layup tests to date have provided data on the accuracy and precision of the machine, where positional accuracy has been repeatable up to ±2mm without the use of adhesive. The machine was generally shown to be capable of laying up dry fiber glass on a mold with three dimensional geometry while avoiding out-of-mold deformation (waves). Going forward, the deposition rate could easily exceed manual layup rates while holding much tighter positional tolerances. Although the current system is designed to handle up to 280mm fabric, the fundamental method of shifting is not theoretically limited to any panel width; this is notably different than the narrow tapes used in current automated tape layup systems.

3.6 Future Work

Future work will be required to provide proper tool path planning to accurately plan the shifter head manipulations and positioning for 3D layups. This is similar to the planning required for NC code generation in the machine tool industry, but will be complicated by the nature of the flexible fabric as a medium, as opposed to rigid tools and metal stock materials. A closed loop robotic control method will be required to achieve high accuracy. While this work has demonstrated a successful application on deforming and laying up fabric, future work should explore more of the influence of fabric's mechanical properties such as tow deformation, fabric shear force, and locking shear angle.

3.7 Acknowledgement

Research was supported by the Advanced Manufacturing Innovation Initiative (AMII), with funding from the US Department of Energy, TPI Composites, and the State of Iowa, including research teams at TPI Composites, Sandia National Laboratories and Iowa State University. In addition, the research was supported by summer REU (Research Experience for Undergraduates) student assistants by the National Science Foundation under Grant No. EEC 1069283 and a grant from the NSF I/UCRC consortium (WindSTAR). Any opinions, findings, and conclusions or recommendations expressed in this material are those of the author(s) and do not necessarily reflect the views of the National Science Foundation, DOE, TPI or Sandia National Laboratories.

3.8 References

[1] Caduff M, Huijbregts MAJ, Althaus H-J, Koehler A, Hellweg S. Wind Power Electricity: The Bigger the Turbine, The Greener the Electricity? Environmental Science & Technology. 2012;46(9):4725-33.
[2] SIEMENS. Wind turbine with the world's largest rotor goes into operation. 2012.
[3] Abraham D, Matthews S, McIlhagger R. A comparison of physical properties of glass fibre epoxy composites produced by wet lay-up with autoclave consolidation and resin transfer moulding. Composites Part A: Applied Science and Manufacturing. 1998;29(7):795-801.

[4] Debout P, Chanal H, Duc E. Tool path smoothing of a redundant machine: Application to Automated Fiber Placement. Computer-Aided Design. 2011;43(2):122-32.
[5] Gardiner G. A350 XWB update: Smart manufacturing. High- Performance Composites: Gardner Business Media, Inc.; 2011.
[6] Lukaszewicz DHJA, Ward C, Potter KD. The engineering aspects of automated prepreg layup: History, present and future. Composites Part B: Engineering. 2012;43(3):997-1009.
[7] Crossley R, Schubel P, Warrior N. Automated Tape Layup (ATL) of Wind Energy Grade Prepreg Materials. 2010 European Wind Energy Conference & Exhibition2010.
[8] MAG. MAG introduces new VIPER® gantry fiber placement system for supersize wind energy and aerospace parts – first unit acquired by Astraeus Wind Energy. 2012.
[9] Black S. Automating wind blade manufacture Composites Technology2009.
[10] Stephenson S. Wind blade manufacture: Opportunities and limits. Composites Technology2011.
[11] Serrano JCWJC. Composite Materials for Wind Blades. 2010.
[12] Kordi MT, Husing M, Corves B. Development of a multifunctional robot end-effector system for automated manufacture of textile preforms. Advanced intelligent mechatronics, 2007 IEEE/ASME international conference on: IEEE; 2007. p. 1-6.
[13] Kim BC, Potter K, Weaver PM. Continuous tow shearing for manufacturing variable angle tow composites. Composites Part A: Applied Science and Manufacturing. 2012;43(8):1347-56.
[14] Kim BC, Weaver PM, Potter K. Manufacturing characteristics of the continuous tow shearing method for manufacturing of variable angle tow composites. Composites Part A: Applied Science and Manufacturing. 2014;61(0):141-51.
[15] Kim BC, Weaver PM, Potter K. Computer Aided Modelling of Variable Angle Tow Composites Manufactured by Continuous Tow Shearing. Composite Structures. 2015(0).
[16] Magnussen CJ. A fabric deformation methodology for the automation of fiber reinforced polymer composite manufacturing. Ames: Iowa State University; 2011.
[17] McBride TM, Chen J. Unit-cell geometry in plain-weave fabrics during shear deformations. Composites Science and Technology. 1997;57(3):345-51.
[18] Potluri P, Sharma S, Ramgulam R. Comprehensive drape modelling for moulding 3D textile preforms. Composites Part A: Applied Science and Manufacturing. 2001;32(10):1415-24.
[19] Yu W-R, Harrison P, Long A. Finite element forming simulation for non-crimp fabrics using a non-orthogonal constitutive equation. Composites Part A: Applied Science and Manufacturing. 2005;36(8):1079-93.
[20] Yu JZ, Cai Z, Ko FK. Formability of textile preforms for composite applications. Part 1: Characterization experiments. Composites Manufacturing. 1994;5(2):113-22.
[21] Potluri P, Perez Ciurezu DA, Ramgulam RB. Measurement of meso-scale shear deformations for modelling textile composites. Composites Part A: Applied Science and Manufacturing. 2006;37(2):303-14.
[22] Nguyen M, Herszberg I, Paton R. The shear properties of woven carbon fabric. Composite Structures. 1999;47(1–4):767-79.
[23] FUJI. LX-30 High speed 3-axis gantry robot. FUJI Machines; 2011.
[24] CMA/Flodyne/Hydradyne. High Speed Gantry - CMAFH eNewsletter. 2013.
[25] Wang J, Page JR, Paton R. Experimental investigation of the draping properties of reinforcement fabrics. Composites Science and Technology. 1998;58(2):229-37.

CHAPTER 4 COMPUTER-AIDED PROCESS PLANNING FOR AN AUTOMATED COMPOSITE FABRIC LAYUP SYSTEM

A paper prepared for submission to a scholarly journal

Siqi Zhu[1], Matthew C. Frank, PhD[2], Frank E. Peters, PhD[2]

The Wind Energy Manufacturing Laboratory

Department of Industrial and Manufacturing Systems Engineering

Iowa State University, Ames, IA 50010

Abstract

This paper presents the development of a Computer Aided Manufacturing approach that can generate the tool path and motion control parameters for a new composite fabric layup system. The system is intended for broad-loom composite fabric used in large scale composite and is driven by a geometric model of the tooling surface. The specific process uses a *shifting* method of fabric manipulation, where the fabric is sheared along the warp tows by fixing the weft tows via temporary constraints. The process planning consists of two main portions: 1) a method to generate the tool path, and 2) a method to control the machine to execute the tool path. Starting from the mold geometry, a shifted fabric flat pattern is generated. Next, the shifting motion and the deposition motion are planned based on the flat pattern and the mold geometry model. The motion is then converted to machine control code which can be loaded into the machine

---

[1]Primary researcher and author
[2]Authors for correspondence

controller to execute an automated layup. This approach is analogous to Computer Numerical Controlled (CNC) machining, where Numerical Control (NC) code from a Computer-Aided Design (CAD) model is generated to drive the milling machine. Layup experiments utilizing the proposed method were conducted to validate the performance using a large robotic gantry and custom end-effector for shifting. The results show that the process planning software requires minimal time and human intervention and can generate tool paths leading to accurate composite fabric layups.

Keywords

Composites, Automated Layup, Fiberglass, Computer Aided Manufacturing.

4.1 Introduction

This work is based on a new composite fabric *shifting* machine that is was motivated by a need for broad loom fabric layup, specifically, for the layup of fiberglass composite wind turbine blades [1]. The machine is based on a deformation method referred to as *shifting*, which allows the fabric to conform to a curved mold or path. The machine can effectively lay up fabric onto complex three-dimensional (3D) mold geometries (Figure 1). An effective process planning methodology needs to be developed to automate the offline programming for the machine. The method needs to be able to read a geometry description of the desired fabric path, analyze it and generate tool path and machine control code for the machine to lay up the fabric. The algorithm should be automated and require minimal human intervention, similar to Computer-Aided Manufacturing (CAM) software for CNC machining. This paper discusses the development of such a path planning method and detailed process control considerations for the fabric shifting machine. Actual layup tests have been performed using the proposed methodology. The results will be analyzed and discussed in this paper.

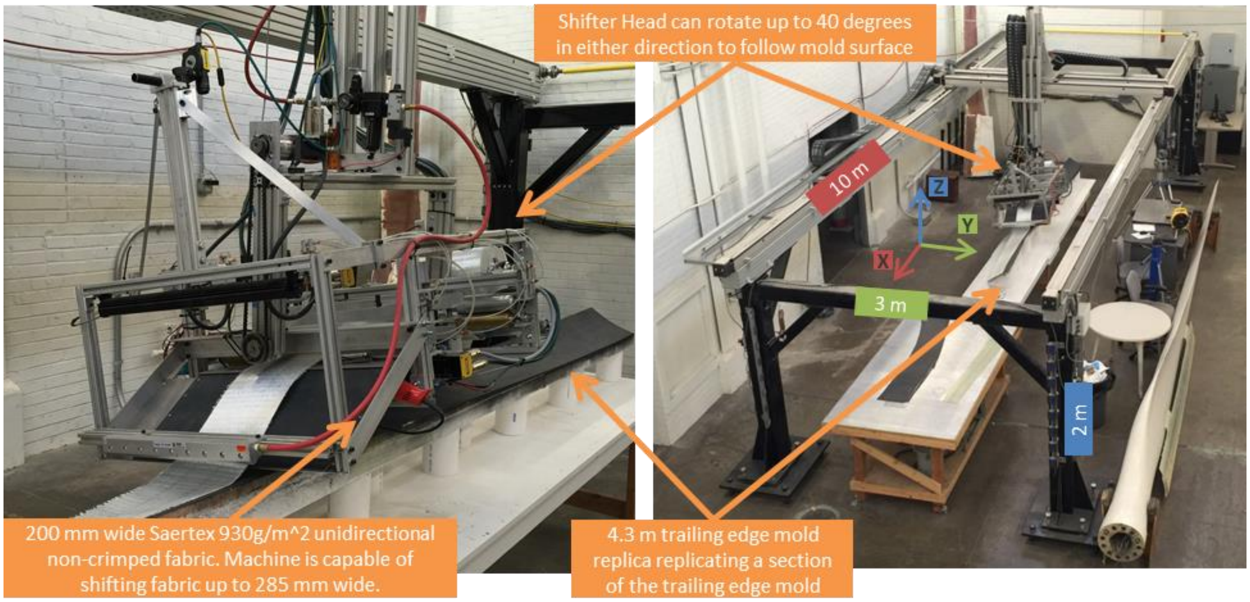

Figure 1. Shifting machine head (left) and the 10 m × 3 m × 2 m gantry system (right).

4.2 Literature Review

Automated composite layup technologies have been developed for various applications. Automated Tape Layup (ATL) and Automated Fiber Placement (AFP) are two popular automated layup technologies that have been widely adopted in the aerospace composites industry [2]. An AFP machine places composite fiber as preimpregnated (prepreg) fabric tapes (ATL) or prepreg slices (AFP) by an end effector attached to a motion system such as a robot arm or a gantry robot. The motion is Computer Numerically Controlled (CNC), and the machine head can follow predefined 2D or three dimensional 3D courses to lay fiber tows onto the desired positions. Sloan gave an overview on AFP and ATL in 2008, focusing mainly on industrial applications such as the use of AFP on the Boeing 787 manufacturing [3]. Lukaszewicz et al.

provided a very thorough synopsis on the past publications on ATL and AFP [4]. AFP generally places low areal weight prepreg tows, which limits it to aerospace applications [4]. One reason is that the tackiness of the prepreg material is needed for the material to be attached to the mold or the previous layer. On the other hand, the shifting machine lays up a complete fiberglass fabric ply comprising multiple tows. For example, the E-glass used in the shifting experiments is 200 mm wide and has 56 tows. The advantage of laying up a fabric ply is that we can achieve better production rate (weight per unit time) with the same machine deposition speed. The down side is that the wider fabric can be more difficult to adapt to the mold shape than the individual AFP tows in the case of complex mold geometries. Traditional AFP can only steer a tow across a turn by forcing the tows to shear by the rotation of the end effector [5]. Defects such as tow wrinkling and folding may occur when the radius is too tight. To solve this problem, Kim et al. developed the Continuous Tow Shearing (CTS) method manufacture variable angle tow (VAT) composites, and the deformation mechanism was quite similar to the shifting method [6]. They followed the initial development of the CTS process by investigating the manufacturing characteristics [7] and the development of a computer aided modelling method [8]. Tool path planning for AFP and ATL is typically in the form of offline programming which consists of two main steps: 1) Generate an initial path according to the geometric design of the part. 2) Offset the initial path to cover the entire mold surface [9]. Shirinzadeh et al. reviewed the existing path planning methodologies in AFP and gave their own approach in 2007 [10]. Offline programming algorithm for AFP considers various factors such as part geometry, fiber orientation, material steering limit, overlag/gap allowance, course width, collision avoidance, etc.[11]. Hasenjaeger compared today's offline programming for AFP to the early stage of CNC metal cutting development when offline programming was machine dependent, technology was expensive and technology advancement was slow [12]. VERICUT Composite Programming (VCP) developed by CGTech is one of the leading AFP process planning packages commercially available [12]. Because AFP and ATL do not involve fiber shifting and many other differences from the shifting based layup machine, their path planning algorithm cannot be directly applied to the shifting machine.

Another popular CNC controlled automated layup method is filament winding during which composite fiber is wrapped around a mandrel to form the desired shape [13, 14]. However, the path planning method of filament winding cannot be applied to the shifting machine because the application of filament winding is limited to cylindrical structures such as pressure vessels and pipes [15].

The tool path planning of the shifting machine is somewhat analogous to the tool path planning for CNC machining which has become a mature process after decades of studies and improvements. Cutter Location point (CL) and Cutter-Contact point (CC) are two important concepts in CNC machining. As shown in Figure 2 by Yau et al., the CL point is the a point on the centerline of the tool and the CC point is where the tool make contact with the part[16].

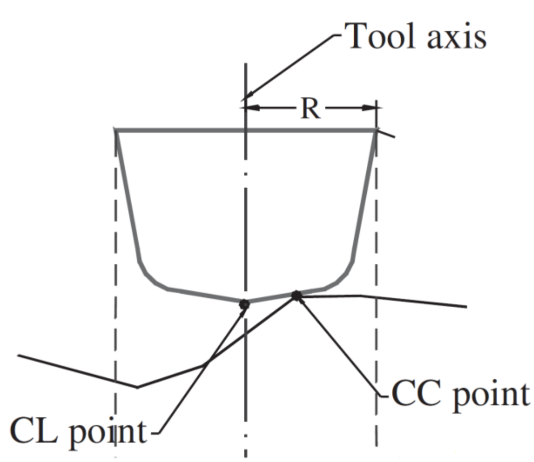

Figure 2. CL point and CC point.[16]

CL path and CC path are different due to the radius and shape of the tool. Figure 3 by Hwang and Chang [17] illustrates an example where CC path follows the desired cutting contour while CL is generated from the CC path. To plan the path for a NC machining process, the CAD model is used to generate CC data since it is how the metal will be cut. Next, CL path is generated from the CC with a process generally known as cutter radius compensation [18]. Other factors such as tool deflection, collision avoidance are also considered in CNC path planning [18-20].

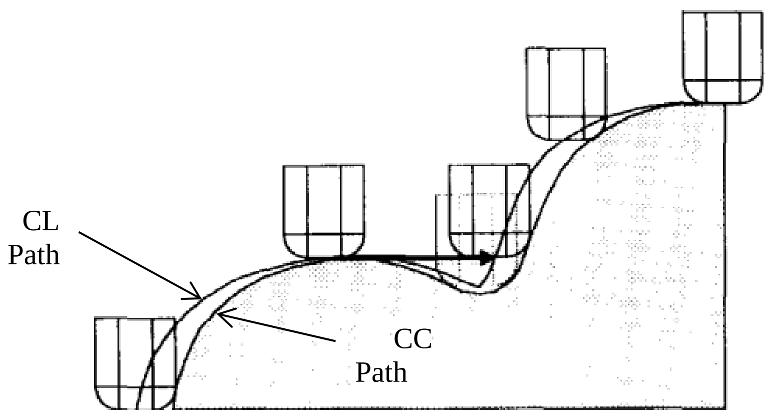

Figure 3. CL path is typically generated from the CC path.[17]

The path planning for the shifting machine is analogous to CNC machining because the *Fabric Contact Point (FC)* where fabric meets the mold can be considered something like a Cutter Contact point while the position and orientation of the machine head, referred to as *Machine Location (ML)* can be thought of as the Cutter Location of a CNC machine. FC points can be generated from a desired fabric path. ML can then be derived from the FC points and other factors such as mold geometry, fabric geometry, collision avoidance, etc.

Classical robotics theories were used to model and control the shifting machine. Specifically, Denavit–Hartenberg notation [21] was used to model the kinematics of the machine which makes the kinematic model standardized and easy to expand.

4.3 Kinematic Modeling of the Fabric Shifting Machine

The layup process is performed by the shifting machine head attached to a three-axis gantry robot. The motion system consists of three linear axes (referred to as X, Y and Z axis) orthogonal to each other and a rotational axis referred to as A axis on the shifter head provides a roll motion about the X-axis. Thus, the machine has a total of four degrees of freedom, as seen in

Figure 4. A mathematical model will be derived to describe the kinematics of the shifting machine.

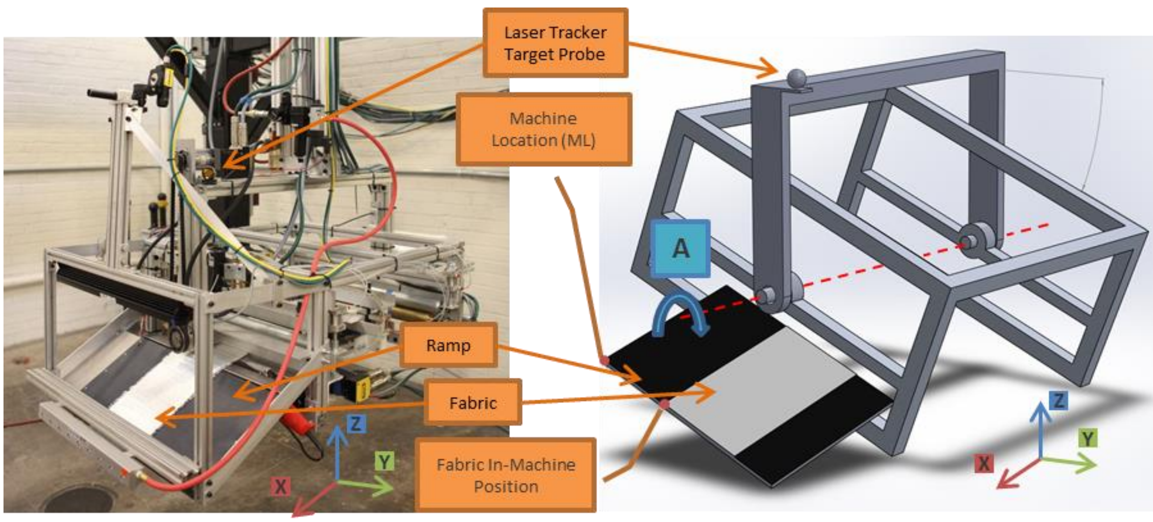

(b)

(a)

Figure 4. Actual picture (a) and schematic (b) of the shifting head showing freedom of movement of the shifting machine.

Machine Coordinate System

A Machine Coordinate System (MCS) is constructed based on the direction of the three physical axes of the gantry system. A FARO Laser Tracker target probe was placed onto a nest fixed on the gantry extension down from the gantry's carrier(

Figure 4). The location of the probe center is regarded as the origin of the MCS when the machine is at its home position, which is defined by the home switches on the machine's three axes. The positive X direction of the MCS is parallel to the gantry machine's positive physical X axis. Similarly, the positive Y direction of the MCS is parallel to the machine's positive Y axis and Z axis is parallel with the machine's Z axis (Figure 5). This MCS was virtually defined in the FARO CAM2 Measure 10 software so that the position of the machine can always be measured or verified by a FARO coordinate measurement machine (CMM). Note that as the machine is performing a layup, it is generally travelling in the negative X direction. As a convention, the front of the machine is referred to the side with the fabric roll attached. The rear is referred to the side with the black deposition ramp.

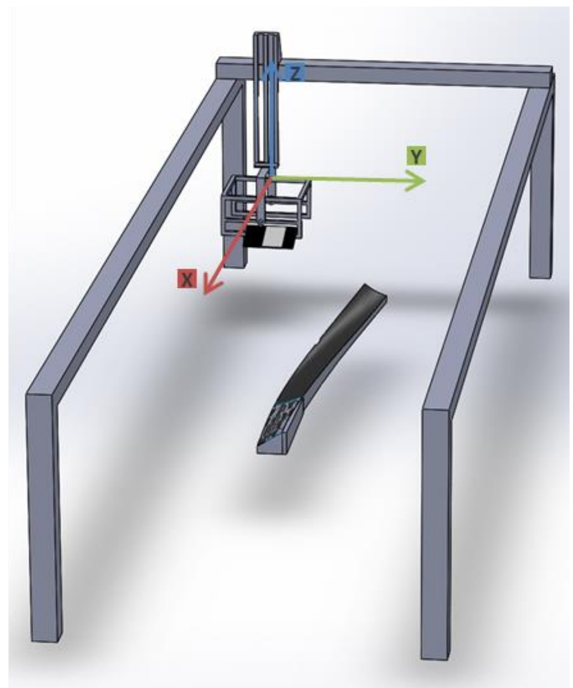

Figure 5. The origin and direction of the Machine Coordinate System shown in an actual picture (left) and a schematic (right).

Forward Kinematics

The Denavit–Hartenberg notation [21] with convention explained by Craig [22] was used to represent the kinematic model. In this model, each of the four motion axes is regarded as a joint of a robot. Each of the gantry's three linear motion axes is a prismatic joint. The rotational axis for the shifter head is a revolute joint. The position and orientation of the lower left ramp corner is used to represent the Machine Location, ML (Figure 4b). The transformation matrices from the origin of the MCS to ML are shown as follows:

$$^{0}T_1 = \begin{bmatrix} 0 & -1 & 0 & 0 \\ 1 & 0 & 0 & 0 \\ 0 & 0 & 1 & 0 \\ 0 & 0 & 0 & 1 \end{bmatrix} \quad ^{1}T_2 = \begin{bmatrix} 0 & -1 & 0 & 0 \\ 0 & 0 & -1 & -X \\ 1 & 0 & 0 & 0 \\ 0 & 0 & 0 & 1 \end{bmatrix} \quad ^{2}T_3 = \begin{bmatrix} 0 & -1 & 0 & 0 \\ 0 & 0 & -1 & -Y \\ 1 & 0 & 0 & 0 \\ 0 & 0 & 0 & 1 \end{bmatrix} \quad ^{3}T_4 = \begin{bmatrix} 0 & 1 & 0 & 0 \\ 0 & 0 & -1 & -Z \\ -1 & 0 & 0 & 0 \\ 0 & 0 & 0 & 1 \end{bmatrix}$$

$$^{4}T_5 = \begin{bmatrix} 1 & 0 & 0 & 0 \\ 0 & 1 & 0 & 0 \\ 0 & 0 & 1 & \mathrm{D}_5 \\ 0 & 0 & 0 & 1 \end{bmatrix} \qquad ^{5}T_6 = \begin{bmatrix} \cos(A) & \sin(A) & 0 & \mathrm{a}_5 \\ 0 & 0 & 1 & d_6 \\ \sin(A) & -\cos(A) & 0 & 0 \\ 0 & 0 & 0 & 1 \end{bmatrix}$$

$$^{6}T_7 = \begin{bmatrix} \cos(\theta_7) & -\sin(\theta_7) & 0 & a_6 \\ \cos(\alpha_6)\sin(\theta_7) & \cos(\alpha_6)\cos(\theta_7) & -\sin(\alpha_6) & -\mathrm{D}_7\sin(\alpha_6) \\ \sin(\alpha_6)\sin(\theta_7) & \sin(\alpha_6)\cos(\theta_7) & \cos(\alpha_6) & \mathrm{D}_7\cos(\alpha_6) \\ 0 & 0 & 0 & 1 \end{bmatrix}$$

Thus, ML can be represented as:

$$\begin{aligned} X_{ML} &= d_6 - X + d_7\cos(\alpha_6) \\ Y_{ML} &= Y - a_5 - a_6\cos(A) + d_7\sin(\alpha_6)\sin(A) \\ Z_{ML} &= d_5 + Z + a_6\sin(A) + d_7\sin(\alpha_6)\cos(A) \end{aligned}$$

where X, Y, Z and A are the position of motion axes and the other parameters are due to the inherent design of each link in the shifting machine.

The next joint is at the position of the fabric on the machine ramp. The position of the fabric relative to the ramp is different for each shift when the fabric is being laid onto the ramp. If the fabric position relative to the mold can be measured, the 3D position of the fabric can be derived. This is made possible by a COGNEX machine vision camera. The intersection point between the fabric edge and ramp edge, referred to as the *in-machine position* of the fabric, can be detected by the camera. Figure 4b illustrates the fabric in-machine position in a schematic. Figure 6 shows a picture taken from the vision camera for the ramp surface. Once programmed, the camera can measure the distance from the in-machine position point to the ML point. This length, referred to as L, will be used to obtain the three dimensional coordinate of the fabric in-machine position. The transformation matrix from the ramp edge to the fabric's in-machine position is simply:

$$ {}^{7}T_{9} = \begin{bmatrix} 1 & 0 & 0 & L \\ 0 & 1 & 0 & 0 \\ 0 & 0 & 1 & 0 \\ 0 & 0 & 0 & 1 \end{bmatrix} $$

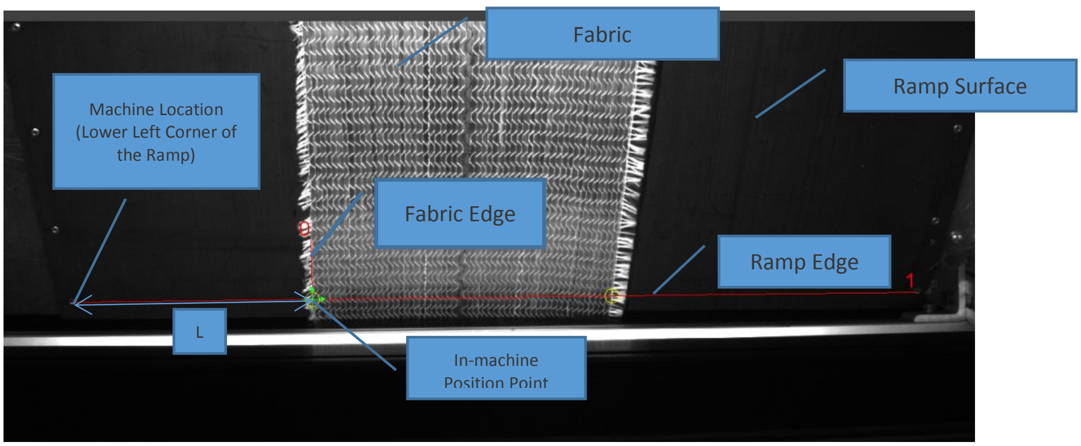

Figure 6. Distance measurement by the Cognex camera. Red line is the ramp edge. L is measured by vision camera.

$$ X_f = X - D_6 - D_7\cos(\alpha_6) - L\sin(\alpha_6)\sin(\theta_7) $$

$$ Y_f = Y + A_5 + A_6\cos(U) + L\cos(\theta_7)\cos(U) + \cos(\alpha_6)\sin(\theta_7)\sin(U) - D_7\sin(\alpha_6)\sin(U) $$

$$ Z_f = Z + L\cos(\alpha_6)\cos(U)\sin(\theta_7) - A_6\sin(U) - D_7\sin(\alpha_6)\cos(U) - L\cos(\theta_7)\sin(U) - D_5 $$

One further step is to predict the Fabric Contact point (FC) where fabric makes contact with the mold. This step can be thought of as working out the Cutter Contact point (CC) by cutter radius compensation in CNC machining. A model is proposed in which the FC is obtained by projecting the in-machine position point down along a certain direction and by a certain distance. The direction and distance are governed by the ramp's slope, the distance between the ramp edge and mold surface and the roll angle. The transformation matrices from the fabric's in-machine position to the on-mold position are:

$$ {}^{9}T_{10} = \begin{bmatrix} 0 & -1 & 0 & 0 \\ \cos(\text{rampAngle}/2) & 0 & \sin(\text{rampAngle}/2) & 0 \\ -\sin(\text{rampAngle}/2) & 0 & \cos(\text{rampAngle}/2) & 0 \\ 0 & 0 & 0 & 1 \end{bmatrix} $$

$$ {}^{10}T_{11} = \begin{bmatrix} 1.0 & 0 & 0 & 0 \\ 0 & \cos(0.4A) & \sin(0.4A) & -\dfrac{h\sin(0.4A)}{\cos(\text{rampAngle}/2)} \\ 0 & -\sin(0.4A) & \cos(0.4A) & -\dfrac{h\cos(0.4A)}{\cos(\text{rampAngle}/2)} \\ 0 & 0 & 0 & 1.0 \end{bmatrix} $$

Where *h* is the vertical distance between the ramp edge and mold surface, *A* is the roll angle of the machine head and *rampAngle* is the angle between the ramp surface and the horizontal plane.

With the forward kinematics, we will be able to calculate ML and FC. ML can be derived from the motion axes position, X, Y, Z and A, while FC needs to be calculated with additional information such as camera measurement results and mold geometry.

Inverse Kinematics

The inverse kinematic model from FC to the fabric in-machine position can be obtained by working backward on the forward kinematic equations. The inverse kinematics from the in-machine position to the X, Y and Z values can be directly solved from the forward kinematic equations algebraically if A and L are known. From on-mold position to the in-machine fabric position:

$$
{}^{11}T_9 = \begin{bmatrix} 0 & \cos(\text{rampAngle}/2) & -1.0\sin(\text{rampAngle}/2) & 0 \\ -\cos(0.4A) & -\sin(\text{rampAngle}/2)\sin(0.4A) & -1.0\cos(\text{rampAngle}/2)\sin(0.4A) & 0 \\ -\sin(0.4A) & \cos(0.4A)\sin(\text{rampAngle}/2) & \cos(\text{rampAngle}/2)\cos(0.4A) & \dfrac{h}{\cos(\text{rampAngle}/2)} \\ 0 & 0 & 0 & 1 \end{bmatrix}
$$

From the in-machine fabric position to the axis positions:

$$X = X_f - d_6 - d_7\cos(\alpha_6) - L\sin(\alpha_6)\sin(\theta_7)$$

$$Y = Y_f + a_5 + a_6\cos(A) + L\cos(\theta_7)\cos(A) + \cos(\alpha_6)\sin(\theta_7)\sin(A) - d_7\sin(\alpha_6)\sin(A)$$

$$Z = Z_f + L\cos(\alpha_6)\cos(A)\sin(\theta_7) - a_6\sin(U) - d_7\sin(\alpha_6)\cos(A) - L\cos(\theta_7)\sin(A) - d_5$$

Where X, Y and Z are the positions of the machine's three axes and X_f, Y_f and Z_f are the coordinate of the fabric's in-machine position.

4.4 Path Planning Method

The shifting machine layup process consists of two parts: 1) deforming the fabric by the clamps' shifting motion inside the machine head, and, 2) depositing the shifted fabric onto the mold by the machine head's deposition motion. In an actual layup, the two processes are mixed together; the machine shifts the fabric first, followed by a deposition and then the next shift followed by another deposition, and so forth. However, the shifting and deposition can be considered as two separate processes for the purpose of tool path generation. The overall path planning methodology is summarized by the flowchart in Figure 7, followed by discussion on the details of this method.

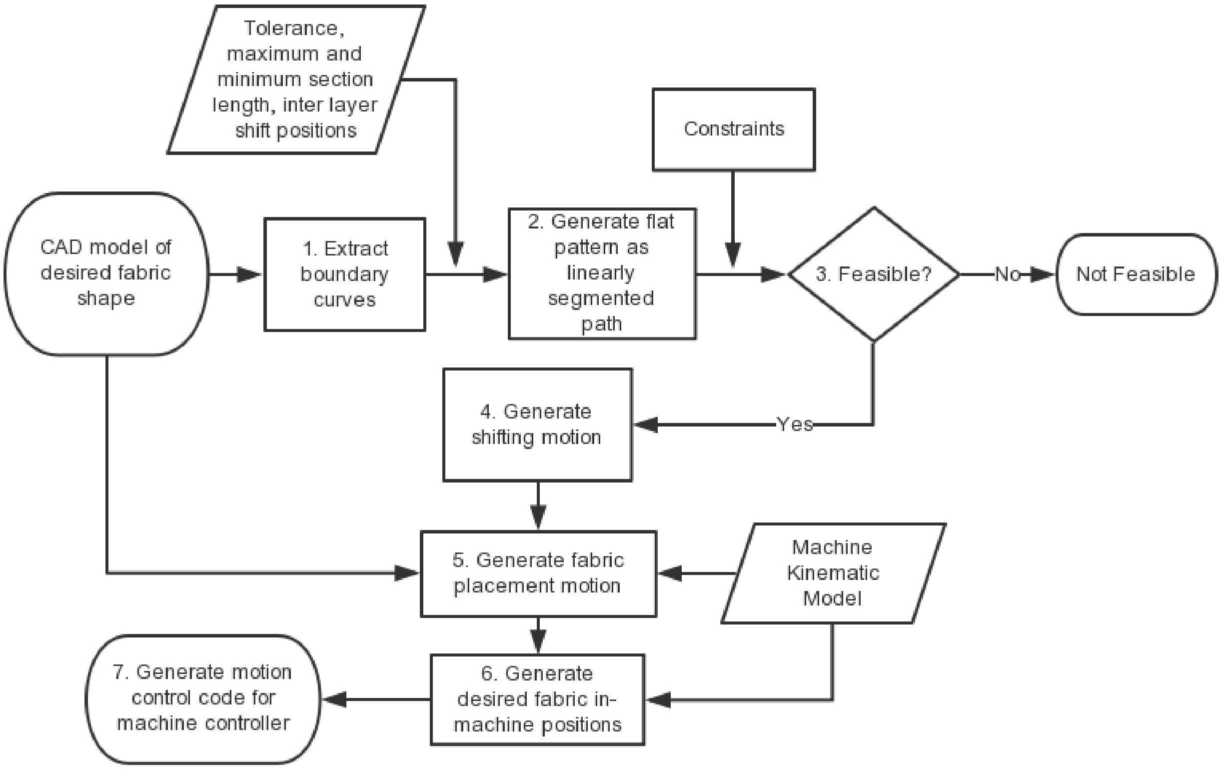

Figure 7 Summary of the path planning methodology.

A flat shifted fabric pattern can be generated by analyzing the geometry of the 3D mold surface. This flat pattern will be used to plan the shifting motion. Then, the depositing motion will be planned to lay the shifted fabric onto the desired position of the mold. After the two parts of the motion are planned, they are combined by the program to generate motion parameters which will leads to motion control codes that the machine controller can read. Details of the path planning methodology are presented in the following sections.

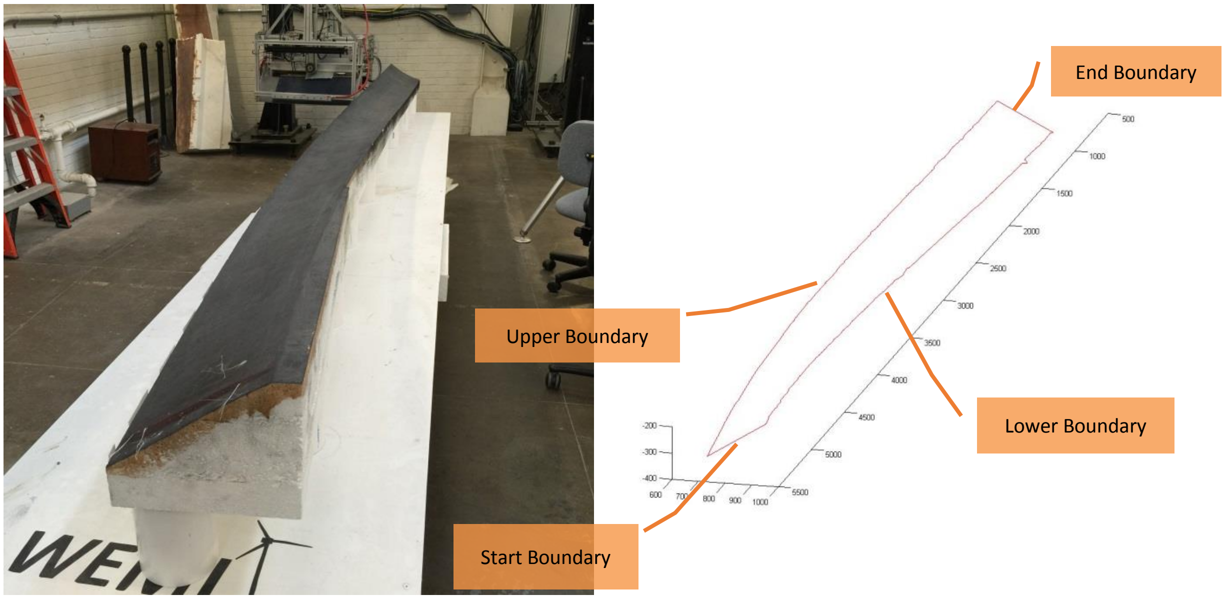

(a) (b)

Figure 8. (a) A mold section for trailing edge layup. (b) The boundary curves measured from the mold.

1) **Extract guide curves from the layup design**. The design of the composite fabric layup is generally defined as a geometric model in a Computer Aided Design (CAD) environment. The layup design can be directly defined in a commercial CAD software package for composite layup such as Fibersim [23]. Alternatively, the geometry can be obtained by a scan/measurement of the mold. No matter what method is used to describe the fabric design, a fabric layer should be described as a surface with four boundary curves. In the context of our application, two of the curves define the start and the end of a fabric layer, and the other two are guide curves that define the path of this fabric layer. In this stage, the four boundaries are extracted and will be used in the rest of the path planning processes. An actual mold surface is shown in Figure 8a, where the boundary layer is measured using a FARO Laser Tracker.

2) **Generate flat pattern**. The shifting process can only generate linearized fabric patterns as discussed in Zhu's work [1]. In this step, the guide curve is fitted with a 3D polyline. How

well the fitted poly line approximates the original curve is measured by the maximum chordal deviation between the fitted line and the guide curve. Each endpoint in the polyline represents a shift location. Each line segment in the polyline represents the warp direction tow on the edge of a shift section. The length of a shift section is controlled by the allowed chordal deviation and the maximum and minimum shift length the machine is capable of. Note that shift locations in different plies may need to be distributed strategically throughout the stack of plies in order to distribute stress concentration and for better shape approximation (i.e.: if we have a shift location on ply “n”, then we should avoid that same location in the “n+1” layer above or “n-1” layer below). Next, a line in the Y-Z plane representing the weft direction tow is attached to each line segment. The weft direction lines are always in the Y-Z plane and parallel to the mold surface. Figure 9 shows the simplified curves (blue) fitted to a scanned guide curve (red), while Figure 10 shows the simplified curve fitted to the entire mold surface.

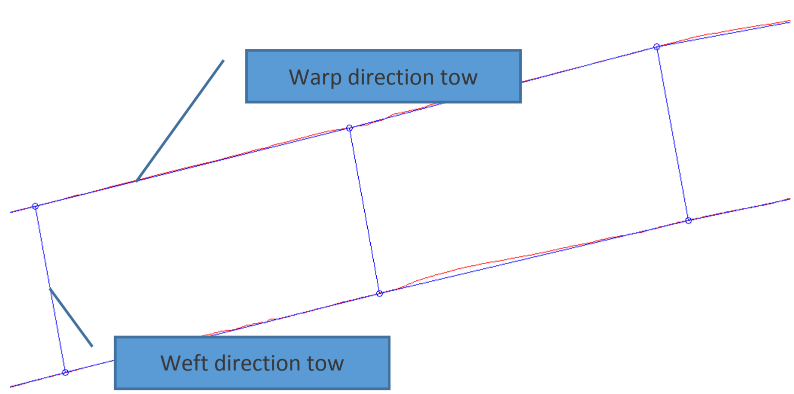

Figure 9. Simplified curve (blue) and guide curve(red).

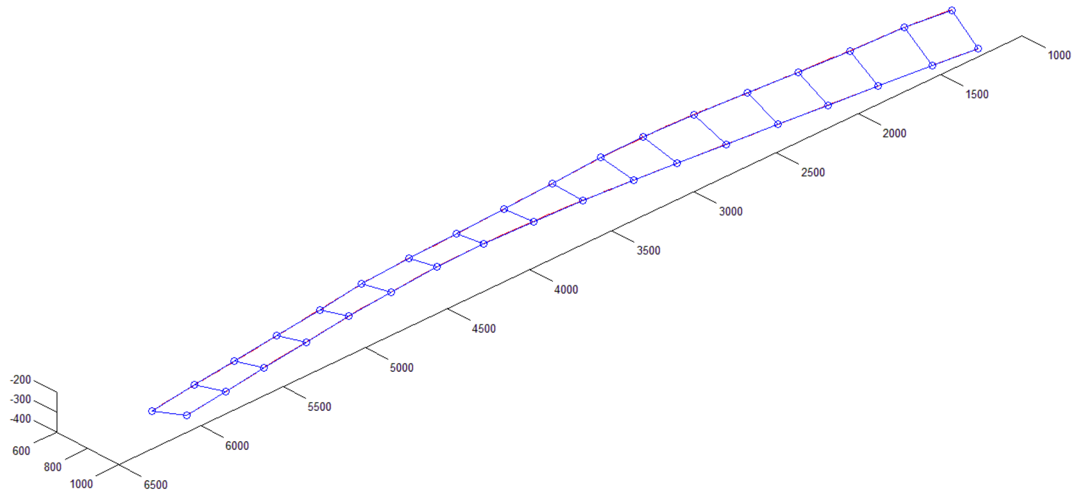

Figure 10. The 3D simplified curve.

Each pair of warp and weft tows can define a parallelogram. This parallelogram is then used to define a shift. By connecting all the shifts together, a flat pattern can be obtained which consists of consecutive parallelogram fabric sections, each sharing two sides with its neighbors (except for the two on the ends), as shown in Figure 11.

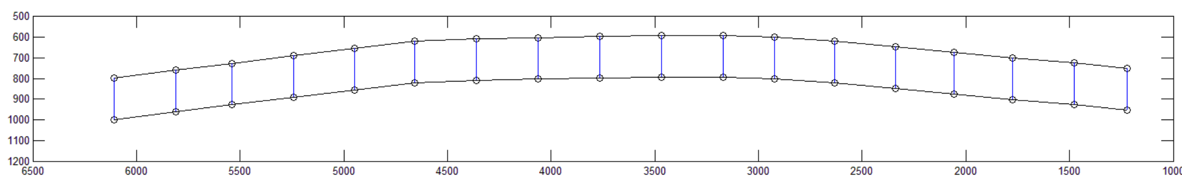

Figure 11. The 2D shifted flat pattern.

The shared sides, referred to as the *base* of a section, are all parallel to the weft direction of the fabric and the length of the shared sides is equal to the width of the fabric, as shown in Figure 12. The other two sides are referred to as the *side* of a section. The orientation of the sides is governed by the shape of the designed fabric path and limited by the shear locking limit of the fabric.

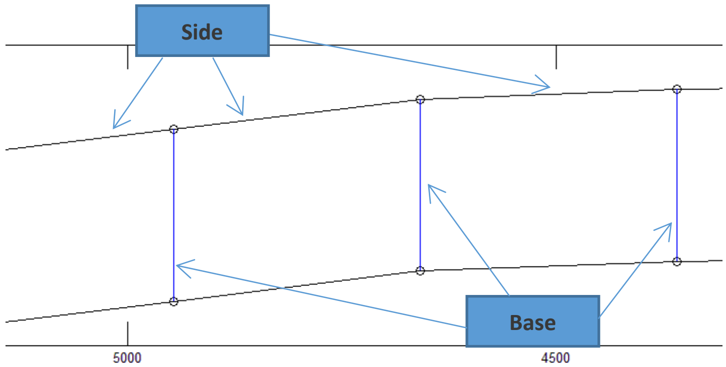

Figure 12. Enlarged view of the shifted flat pattern

3) **Analyze feasibility**. The feasibility of the layup is checked at this stage. Criteria of the feasibility check includes: a) The section size and shifting motion should not exceed the machine's capability, b) The shear angle should not exceed the fabric's shear locking limit, c) The deviation between the actual fabric path and the desired path should be controlled within the tolerance specified by the design, (Note that both process variability and the curve simplification cause the actual fabric path to deviate from the desired path), and finally, d) Undevelopable curvatures too severe for the fabric to conform to the mold must be avoided.

4) **Generate shifting motion**. The shifting motion consists of three steps: 1) the distance between the two clamps is adjusted to be equal to the side length of the shift section, 2) the clamps are closed, and 3) the shifting clamp moves in the weft direction and the spacing clamp moves in the warp direction toward the shifting clamp to create the shift. As shown in Figure 13, the *shift distance* is defined as the displacement of the shifting clamp to create the shift. The *shift length* is defined as the length of the side edges. The *shift height* is the height of the shifted fabric section measured between two bases. As a convention to make the path planning easier to understand, the shift distance is positive when the fabric is deformed to the right side of the layup direction, and negative when deformed to the left side. The

relationship between shear angle, shift length, shift height and shift distance can be described as:

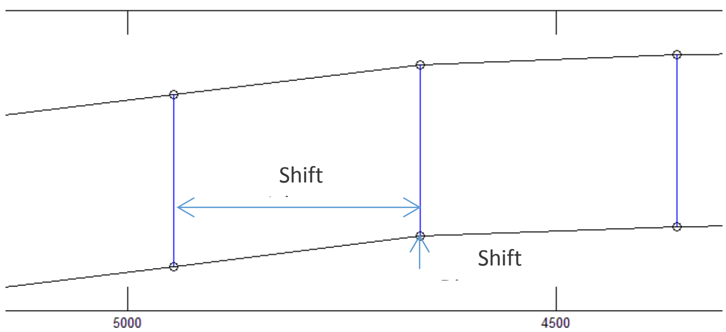

Figure 13. Shifting motion parameters.

Shift distance = cos (shear angle) × shift length

Shift height = sin (shear angle) × shift length

The aforementioned parameters will be calculated and stored to perform shifting motion.

5) **Generate fabric placement motion**. Each time the machine shifts a section, the machine naturally has to stop its deposition motion and move synchronized with the shifting clamps to create the shift. After shifting, the clamps open and the machine moves forward one step to shift the next section. To deposit fabric onto the mold, the machine will do a linear motion whose direction is normal to the base edge of the shifted fabric, otherwise fabric will be steered. The motion should also be parallel to the mold surface under the assumption that the mold surface is locally flat. The length of the motion should be equal to the height of the previously shifted fabric. After the linear deposition motion, the machine head is rotated to make the ramp edge parallel to the mold surface. Figure 14 shows the deposition path in which the black polyline with "+" markers represents the path of the ML and the green lines represent ramp edge where the machine head rotates to a new roll angle.

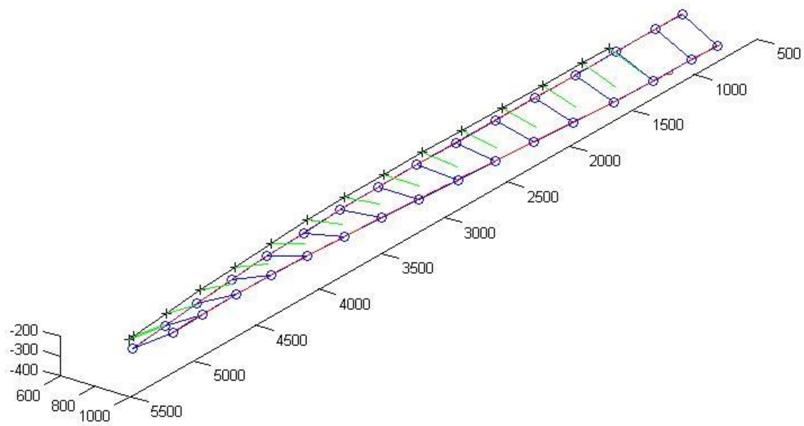

Figure 14. Fabric placement motion represented by the polyline with "+" markers.

6) **Generate fabric in-machine positions**. The theoretical in-machine position each time the machine stops is calculated. When the machine stops to shift fabric, there is a check to see if the fabric's actual in-machine position matches the planned in-machine position (using vision system). If not, the machine will compensate for the error by moving the fabric toward the desired position by a linear motion.

7) **Generate machine control code**. The machine control code is generated based on the machine motions discussed above. The parameters include the motion displacement for each task and step.

4.5 Machine Control Method

The process of laying up a fabric ply consists of different actions including cutting fabric, actuating cylinders for the rollers and clamps to open and close, performing shifting deformation and depositing fabric. The machine control sequence is summarized in the flowchart shown in Figure 15 and discussed in the following section.

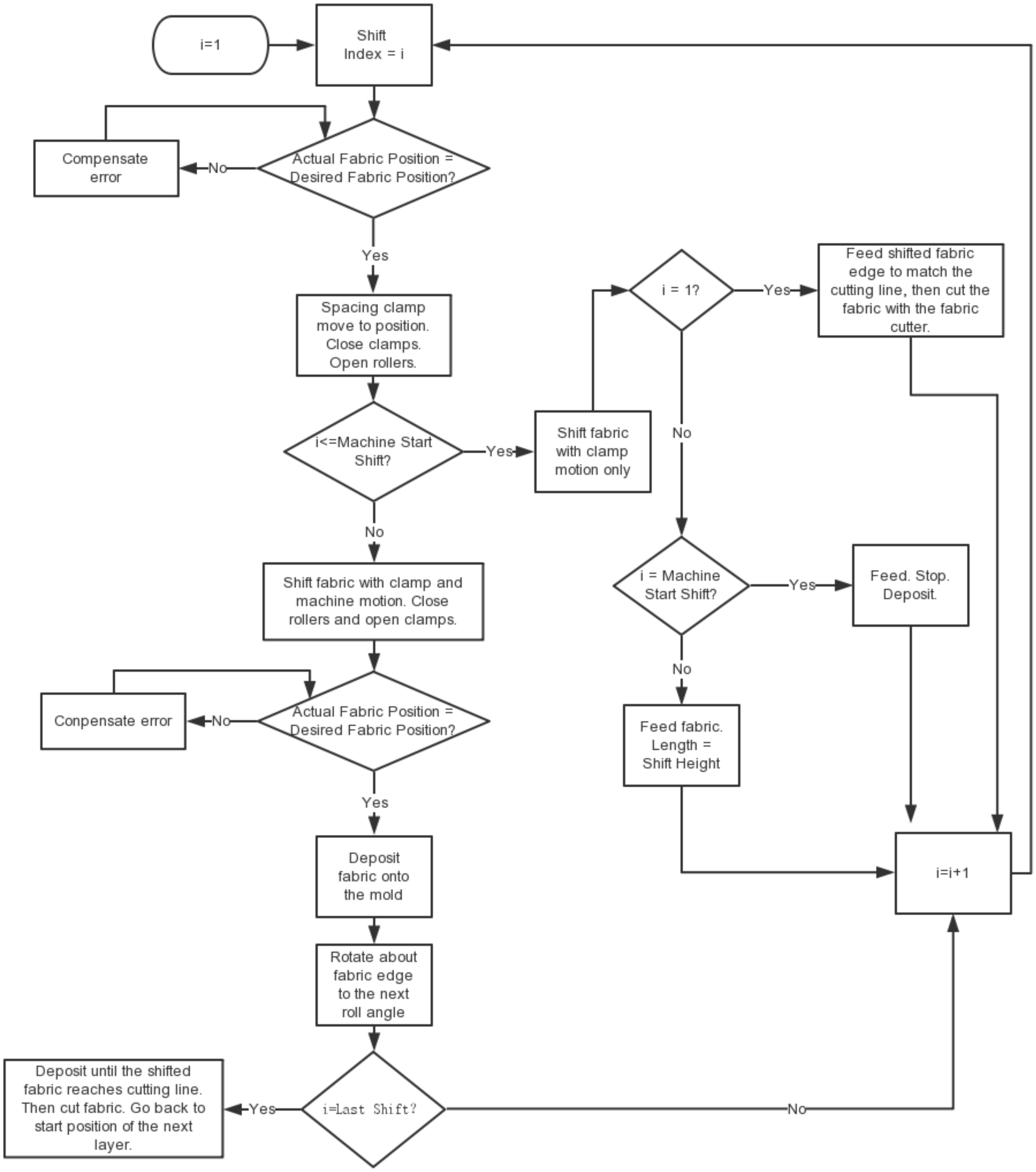

Figure 15. Summary of the machine control methodology.

The shifting routine consists of the following steps:

1) Before the first shift, straight fabric is fed into the machine and between the clamps.

2) Clamps close. Rollers open and the clamps perform a shift.

3) Rollers close. Clamps open and rollers feed the shifted fabric so that the base edge just reaches the cutting line.
4) The cutter will cut off the fabric outside the machine.
5) Machine will continue feeding the fabric to the point that the shifted fabric's front base edge is just matching the shifting clamp edge.
6) The machine will perform the next shift. And the cycles go on until the "Machine Start Shift" is reached.
7) "Machine start shift" is the shift during the deposition of which the fabric will start touching the mold. Before the fabric touches the mold the machine head does not move. Clamps will perform shifting and rollers will feed fabric out onto the ramp but the machine head stays still. After the fabric reaches the mold the machine head moves along the mold as the rollers feed the fabric.
8) After passing the machine start shift, the machine will synchronously move with the clamp so that the shifting clamp holds its position when shifting as if only the spacing clamp is moving to shift the fabric. At the deposition stage the machine moves forward synchronizing with the rollers' motion to deposit fabric onto the mold. The speed of machine head motion and rollers' feed rate must be the same to avoid dragging or pushing the fabric that has been deposited.
9) After the final shift, the edge of the last shift section is positioned on the cutting line and the cutter will perform a cut. Next, the machine will move forward to lay down the shifted fabric and then move back to the starting position of the next ply.
10) The machine checks and corrects positional errors before and after shifting, as can be seen in the process chart.

4.6 Experiment on the Trailing Edge Layup

Experimental Design

The utility turbine blade this paper is focused on has a 39-meter long trailing edge prefabrication comprising a steered and twisted 3D section which makes it one of the most challenging parts to layup. Of this subcomponent, the most extreme challenging 4.3-meter long subsection was replicated in the laboratory for layup experiments, as shown in Figure 8a. The mold geometry was measured by a FARO Laser tracker, represented by polylines as shown in Figure 8b. Path planning was performed on the measured geometry and machine control code was generated for a fabric layuup. After each layup, the actual position of the fabric was measured and recorded. The fabric position was measured at nine locations evenly distributed along the mold. The distance between the fabric edge and the mold edge, referred to as the *Chordwise Position*, was measured as follows: As shown in Figure 16, each measurement location has a reference point and a reference line that is normal to the mold edge. The Chordwise Position at this measurement location is the distance between the reference point and the fabric edge measured along the reference line.

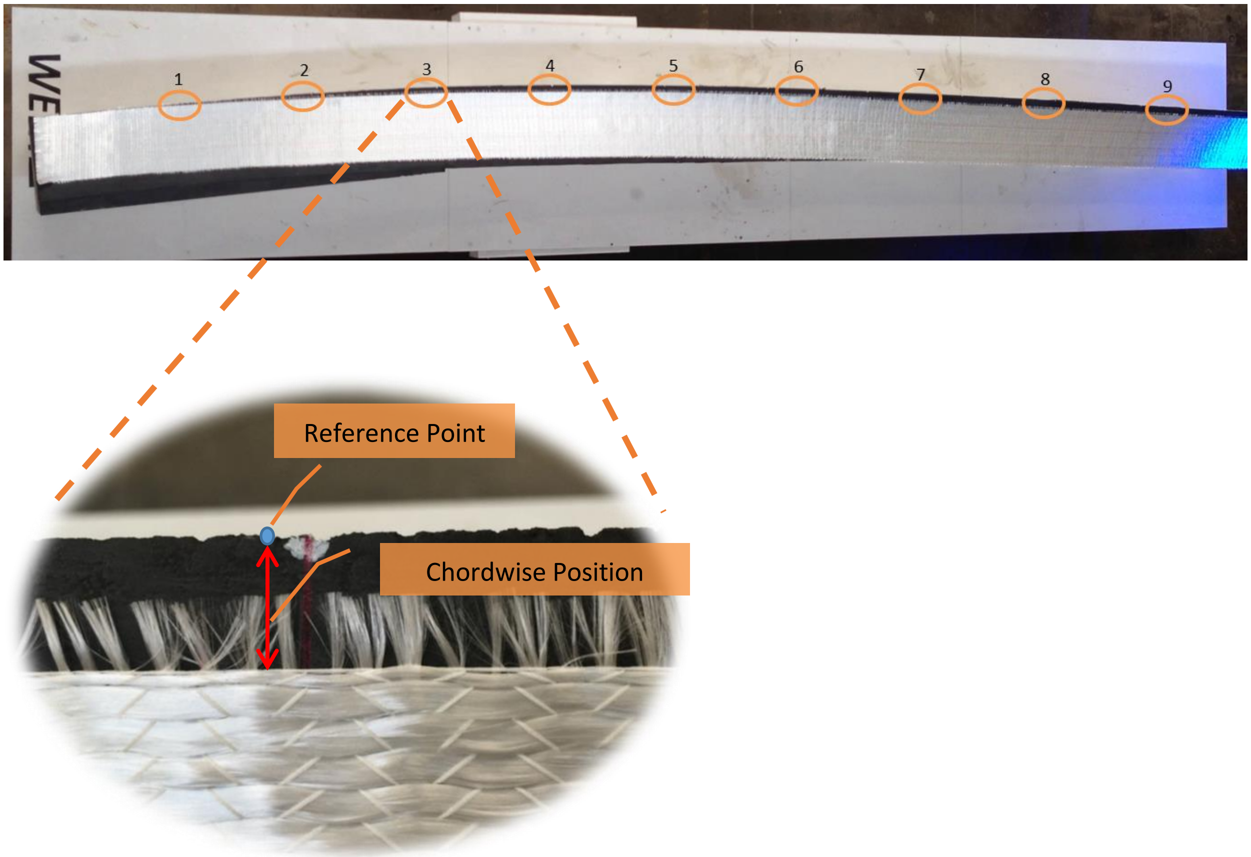

Figure 16. Measurement locations of chordwise position.

Two tests were performed to test the path planning method and program. The first test was focused on characterizing both the positional accuracy and precision of the fabric laid up. In this test, accuracy quantifies how well the mean position of the trials agrees with the desired position while precision quantifies how much positional variability is measured when the same layup is repeated. Hence, five layup trials with identical machine control code were performed. The desired Chordwise Position is 10 mm along the entire length.

The second layup test imitated the chordwise ply drop that is frequently found in the actual layup designs in wind blades manufacturing, where plies of fabric do not entirely overlap each other but stagger on each other with a small offset, as can be seen in Figure 17. This test will show the ability of the path planning method to create multiple layer layups with ply drops.

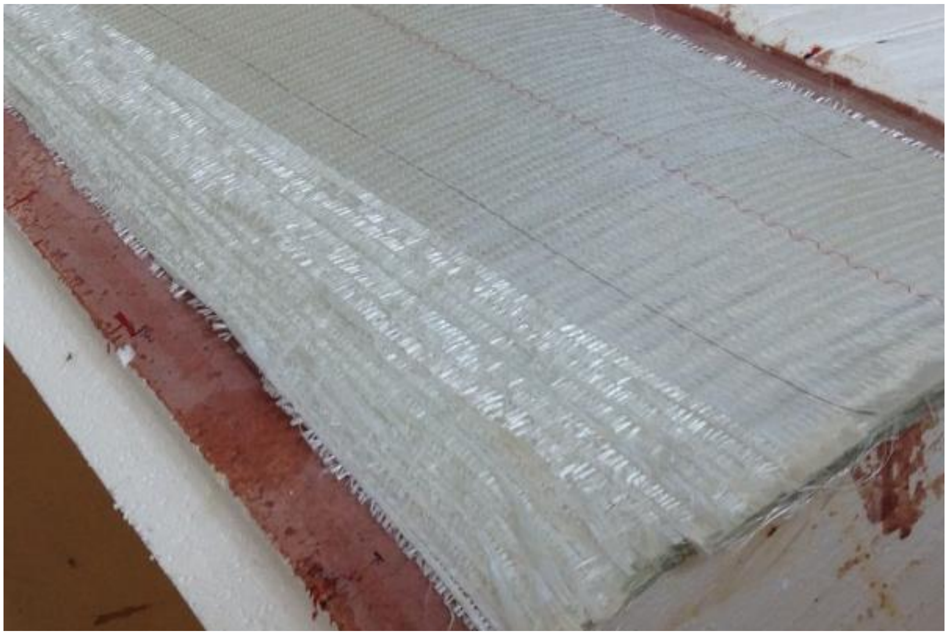

Figure 17. Plies staggered on top of each other, known as "ply drop".

Six different layup paths were generated and used to plan six different layups where the chordwise position of each layer is three millimeters offset from the previous layer (e.g.: the first ply is 10 mm along the entire length, second ply is 13 mm, third ply is 16 mm and so forth). In this experiment, each ply was laid up directly on the mold to make the condition of each layer as similar as possible, minimizing variability.

Results and Discussion

Table 1 summarizes the layup results at each measurement location. Process Capability can be used to quantify how well the process is meeting the desired tolerance [24]. Specifically, the higher the Process Capability means the process is more within the desired tolerance zone. It is defined as:

$$C_{pk} = \min\left[\frac{USL-\mu}{3\sigma}, \frac{\mu-LSL}{3\sigma}\right] \quad [24]$$

where μ and σ are population mean and standard deviation, *USL* and *LSL* are the upper and lower specification limits, respectively. In the context of this test, *USL* is 15 mm and *LSL* is 5 mm.

The sample estimators of the Process Capability was calculated as

$$\hat{C}_{pk} = \min\left[\frac{USL-\bar{x}}{3s}, \frac{\bar{x}-LSL}{3s}\right] [24]$$

Where $\bar{x}$ and s are sample mean and standard deviation, respectively.

Table 1. Results of the repeatability test (mm).

Measurement Location	1	2	3	4	5	6	7	8	9
Mean (mm)	10.52	12.19	11.23	7.66	7.76	10.81	14.23	13.14	10.31
Std (mm)	1.54	1.21	1.02	1.01	1.12	1.03	0.94	1.33	1.29
Lower 95% PI	7.45	9.76	9.19	5.63	5.52	8.74	12.35	10.48	7.73
Higher 95% PI	13.60	14.61	13.28	9.69	10.00	12.87	16.12	15.79	12.88
Ste	0.69	0.54	0.46	0.45	0.50	0.46	0.42	0.59	0.58
Lower 95% CI	9.06	11.03	10.26	6.69	6.69	9.82	13.33	11.87	9.08
Higher 95% CI	11.99	13.34	12.21	8.63	8.83	11.79	15.13	14.40	11.54
Cpk	0.97	0.77	1.23	0.87	0.82	1.35	0.27	0.47	1.21

The result for the repeatability analysis is also shown in Figure 18 as a chart, where the X axis represents the measurement location and the Y axis represents the Chordwise Position. We can see that each ply generally followed a similar pattern. Fabric tends to be closer to the edge than desired at location 4 and 5 whilst the fabric tended to be further away from the edge than desired at other locations. One factor that may cause the different response at location 4 and 5 might be that the shift direction changes at location 4 and 5. As shown in Figure 16, fabric was shifted toward the negative Y direction before location 4, and was shifted toward the positive Y direction after location 5.

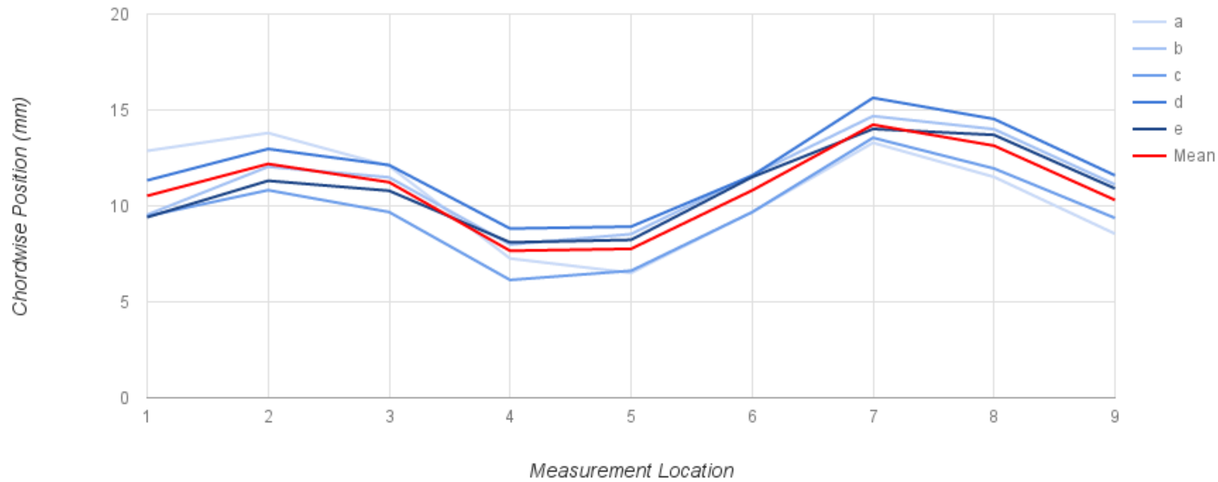

Figure 18. Repeatability test results.

A Gaussian process model was fitted to the experiment data to give prediction interval for the future layups. As shown in Figure 19, the red lines illustrate the 95% prediction interval for future layups. The algorithm used was the *mlegp* package developed by Dancik [25] which provided a maximum likelihood of Gaussian process for the layup data. This model could predict the uncertainty for future layups better than the individual prediction intervals listed in Table 1 because it took the correlation between different measurement locations into account.

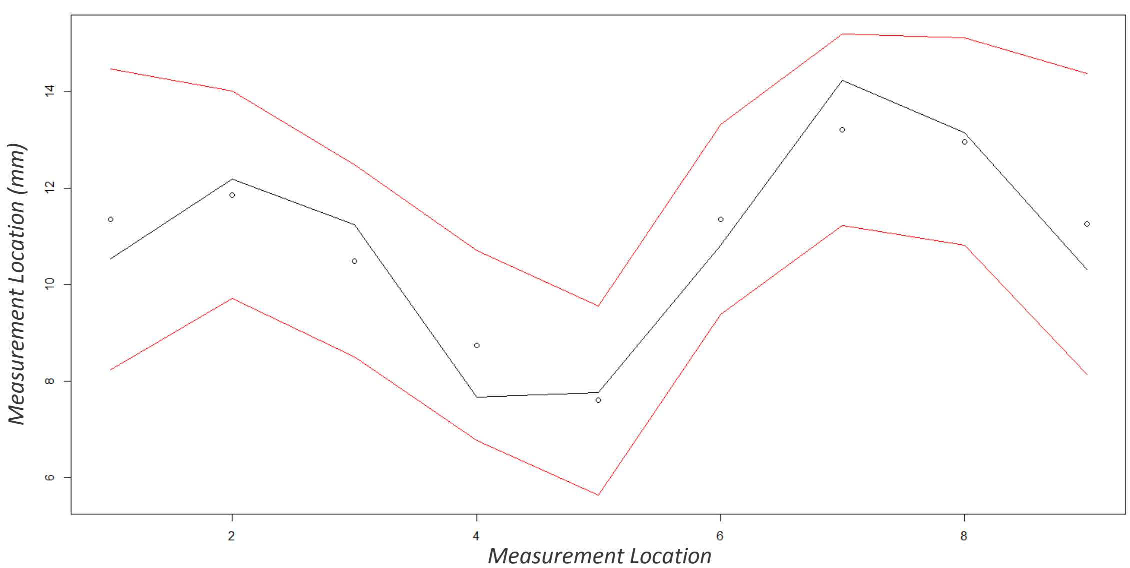

Figure 19. Maximum likelihood prediction for future layups with a Gaussian process model.

The positioning variability could come from various resources. For instance, the fabric rolls used for the layup do not have consistent edge (the fabric is not rolled up exactly into a cylinder from the factory), or the fabric deformation may vary even for the exact same machine motion, due to the inherent flexibility and shearing stiffness variability along the fabric. The width of 95% prediction interval found at each location indicates that the fabric position could be controlled within five millimeters 95% percent of the time. Considering the tolerance for the chordwise position is ±5 mm, this could fulfill the design requirement if the mean position is acceptable.

The result for the offset layup is shown in Figure 20. There were few overlaps between layers. However the offset was not maintained very well due to the variability of the process. The offset layup could be improved by generating better paths for the layers and reducing system error in the layup process. Although the general tolerance for chordwise position was given as ±5 mm, the layups sometimes also require a gradually reducing chordwise distance between layers. To maintain this requirement the layup accuracy needs to be significantly improved.

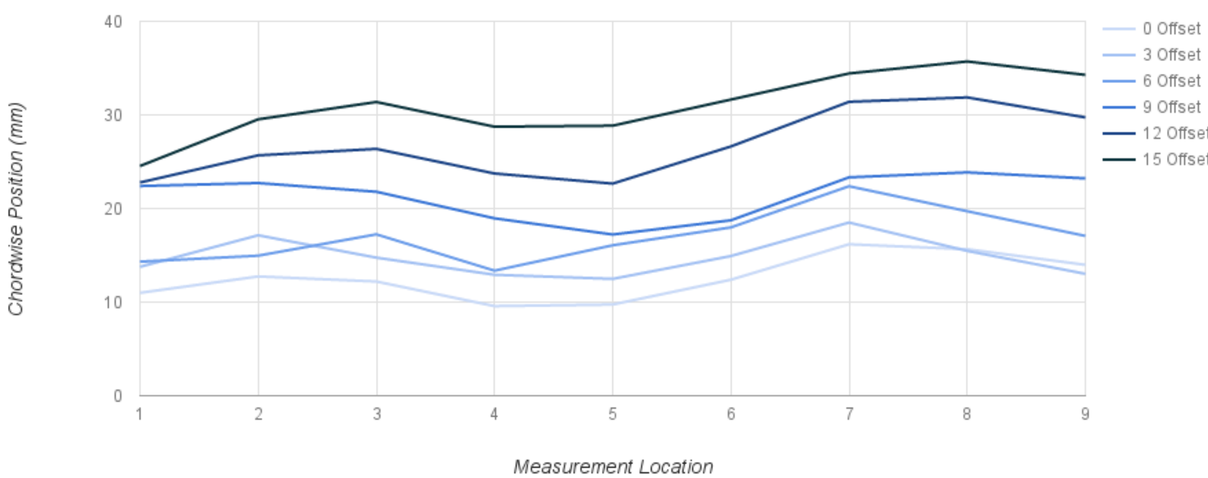

Figure 20. Results for the offset layup.

4.7 Conclusion and Future Work

A process planning algorithm for the fabric shifting machine was successfully developed and implemented in software. The computer program reads the geometric model of a desired fabric path and generates the corresponding tool path in the form of machine control code. Motion procedures are carefully planned to ensure the fabric can be accurately positioned in both chordwise and spanwise direction. Layup tests show that the tool path enables the machine to place fabric reasonably close to the desired location although there is still much room for improvement. Future work should be focused on improving accuracy and precision of the layup process, physically. Although the current process planning algorithm is completed by off-line programming, advanced control techniques such as real time line tracing could potentially be used to compensate error dynamically. In wind blade layups sometimes a gradual change of chordwise distance between layers is needed, which requires a very high accuracy. Possible solution should be investigated to ensure that the process can fulfil actual manufacturing requirements.

4.8 References

[1] Zhu S. An automated fabric layup machine for the manufacturing of fiber reinforced polymer composite. Ames, Iowa2013.
[2] Marsh G. Automating aerospace composites production with fibre placement. Reinforced Plastics. 2011;55(3):32-7.
[3] Sloan J. ATL and AFP: Defining the megatrends in composite aerostructures. High-Performance Composites: Gardner Business Media, Inc.; 2008.
[4] Lukaszewicz DHJA, Ward C, Potter KD. The engineering aspects of automated prepreg layup: History, present and future. Composites Part B: Engineering. 2012;43(3):997-1009.
[5] Blom AW, Lopes CS, Kromwijk PJ, Gurdal Z, Camanho PP. A theoretical model to study the influence of tow-drop areas on the stiffness and strength of variable-stiffness laminates. Journal of Composite Materials. 2009.
[6] Kim BC, Potter K, Weaver PM. Continuous tow shearing for manufacturing variable angle tow composites. Composites Part A: Applied Science and Manufacturing. 2012;43(8):1347-56.
[7] Kim BC, Weaver PM, Potter K. Manufacturing characteristics of the continuous tow shearing method for manufacturing of variable angle tow composites. Composites Part A: Applied Science and Manufacturing. 2014;61(0):141-51.

[8] Kim BC, Weaver PM, Potter K. Computer Aided Modelling of Variable Angle Tow Composites Manufactured by Continuous Tow Shearing. Composite Structures. 2015(0).
[9] Debout P, Chanal H, Duc E. Tool path smoothing of a redundant machine: Application to Automated Fiber Placement. Computer-Aided Design. 2011;43(2):122-32.
[10] Shirinzadeh B, Cassidy G, Oetomo D, Alici G, Ang Jr MH. Trajectory generation for open-contoured structures in robotic fibre placement. Robotics and Computer-Integrated Manufacturing. 2007;23(4):380-94.
[11] Hasenjaeger B. Capabilities of Automated Fiber Placement. Composites World.
[12] Hasenjaeger B. Programming and simulating automated fiber placement (AFP) CNC machines. SAMPE JOURNAL. 2013;49(6):7-13.
[13] Lu H. Effects of tape tension on residual stress in thermoplastic composite filament winding. Journal of Thermoplastic Composite Materials. 2005;18(6):496-87.
[14] Mertiny P, Ellyin F. Influence of the filament winding tension on physical and mechanical properties of reinforced composites. Composites Part A: Applied Science and Manufacturing. 2002;33(12):1615-22.
[15] Lossie M, Van Brussel H. Design principles in filament winding. Composites Manufacturing. 1994;5(1):5-13.
[16] Yau H-T, Chuang C-M, Lee Y-S. Numerical control machining of triangulated sculptured surfaces in a stereo lithography format with a generalized cutter. International journal of production research. 2004;42(13):2573-98.
[17] Hwang JS, Chang T-C. Three-axis machining of compound surfaces using flat and filleted endmills. Computer-Aided Design. 1998;30(8):641-7.
[18] Choi B, Jun C. Ball-end cutter interference avoidance in NC machining of sculptured surfaces. Computer-Aided Design. 1989;21(6):371-8.
[19] Kim GM, Kim BH, Chu CN. Estimation of cutter deflection and form error in ball-end milling processes. International Journal of Machine Tools and Manufacture. 2003;43(9):917-24.
[20] Zeid I. Mastering Cad/Cam: McGraw-Hill, Inc.; 2004.
[21] Denavit J. A kinematic notation for lower-pair mechanisms based on matrices. Trans of the ASME Journal of Applied Mechanics. 1955;22:215-21.
[22] Craig JJ. Introduction to robotics: mechanics and control: Pearson Prentice Hall Upper Saddle River; 2005.
[23] SIEMENS. Fibersim: Complete Software Solution for Composites Design and Manufacturing. 2015.
[24] What is Process Capability. Engineering Statistics Handbook.
[25] Dancik GM. Maximum Likelihood Estimates of Gaussian Processes. 3.1.4 ed: CRAN; 2013.

CHAPTER 5 VALIDATION OF THE SHIFTING DEFORMATION

A paper prepared for submission to a scholarly journal

Siqi Zhu[1], Emily L. Judd[2], Matthew C. Frank, PhD[3], Frank E. Peters, PhD[3]

The Wind Energy Manufacturing Laboratory

Department of Industrial and Manufacturing Systems Engineering,

Iowa State University, Ames, IA 50010

Abstract

This paper presents a study of the material properties of composite fabric after being deformed by a process referred to as *shifting*. Shifting is a new deformation method for automated fabric layup processes in manufacturing wind turbine blades [1]. During the shifting, the fabric is subjected to shearing deformation along the 90 degree (weft) direction. Previous studies included implementing the shifting method into a machine and conducting fatigue tests. The final stage of testing considers whether shifting affects the material properties of fiberglass included measuring the dimensions of the individual tows, also known as *meso-scale tow structure*, in key areas of the fiberglass fabric. Tow width was measured, along with tow thickness, and cross-sectional tow area. Tow spacing, as determined by the presence of gaps, and the tow radii of curvature were also measured. These measurements allowed for inspection of the effects of shifting in conjunction with other standard manufacturing processes. Overall, the results show that shifting

---

[1]Primary researcher and author
[2]Undergraduate research assistant and second author
[3]Authors for correspondence

not create deformations like gaps or compressed tows in amounts that would disqualify the method from use in industry. This suggests that shifting could be a viable method for use in automated composite manufacturing.

Nomenclature

Tow: a group of individual fibers, often used in reference to materials such as fiberglass and carbon fiber, where the combination of many tows creates the material fabric.

Unidirectional fabric: fabric in which approximately 90% of tows run in the same direction, the other 10% are stitched perpendicular to provide the structure for the fabric (Figure 1a).

Warp: 0° fabric direction, runs along the tow direction in unidirectional fabric.

Weft: 90° fabric direction, runs perpendicular to the tow direction in unidirectional fabric.

Meso-scale structure: the structural features at the tow level; when speaking of fiberglass fabric, the meso-scale structure is larger than the micro-scale structure of individual fibers, and smaller than the macrostructure, or the bulk fabric.

5.1 Introduction

As the wind energy industry grows, it is even more important to reduce production costs and increase longevity of the wind turbine blade components. One way to accomplish both of these goals is by incorporating more automation in the manufacturing process. Introducing automation into a manufacturing process can significantly improve product quality and reduce labor costs and production time. Automation decreases labor expenses and increases quality due to process uniformity. The task of manufacturing the trailing edge of wind turbine blades could especially benefit from incorporating automation due to the complex geometries involved in the mold. The trailing edge can sometime be created as a separate sub-component and then added into the reminder of the blade mold. In industry, unidirectional fiberglass fabric used to create the trailing edge is deformed by hand to fit the mold curvature. This sometimes leads to wrinkles and gaps in the fabric, both of which can cause voids during the infusion process, leading to a decrease in material strength. Besides the deformation, variability may also be introduced during manual layup. These conditions can have serious impact on the final material properties such as gaps ((b)

Figure 1b), in-plane waviness, wrinkles, or out-of-plane waviness, and the resulting breakage in the composite matrix from uneven resin infusion can lead to compressive failure [2]. This failure could in turn lead to an overall failure in the wind turbine blade, causing severe ramifications in both repair costs and possible damage to other turbine components.

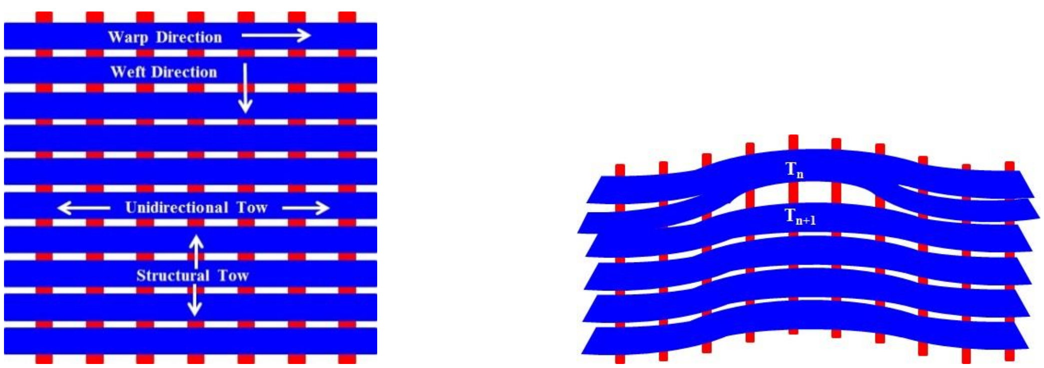

(a) (b)

Figure 1. Unidirectional fabric; (a) terminology defining the tows, and (b) tow spacing in the fabric .

In order to address these issues, Magnussen (2011) proposed a new method for fabric deformation called shifting [1]. This method was used to automate the fabric deformation, as shown in Figure 2. In addition to the automation benefit, the method also decreased unwanted deformations such as wrinkles and gaps as compared with hand-deformed fabric.

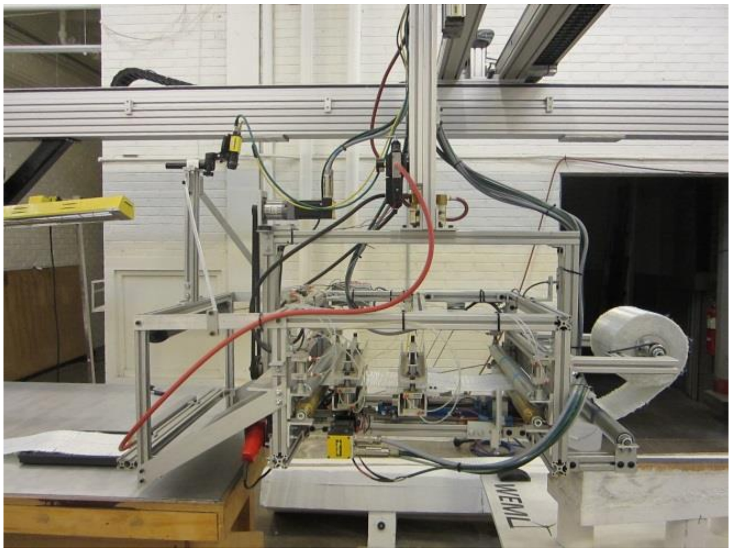

Figure 2. The automated fabric shifting machine.

In this paper, results from an experiment in the final testing stage of the shifting method will be examined. Previously completed studies included implementing the shifting method into an automated machine and running fatigue tests on shifted fiberglass fabric. The current tests look at the tow widths in key areas of interest across shifted samples. These widths were compared to un-shifted control samples. Tow thicknesses for the various areas were also measured and compared to the controls. By examining the change in tow dimensions (Figure 3) caused by the shifting method, it was seen how much in-plane waviness (gaps) and tow compression were introduced to the fiberglass material. The fiberglass samples fabricated in the laboratory to determine if the amount of in-plane waviness and tow compression present in shifted fabric were all within acceptable ranges.

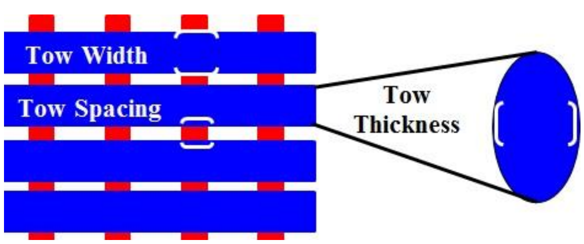

Figure 3. Tow measurement nomenclature.

The overarching purpose of the experiment was to show that shifting is a viable manufacturing method for the production of wind turbine blade trailing edges, as seen in the test shown in (b)

Figure 4b. A full layup test was conducted on industry grad fabric deposited using the shifter system and placed in a production mold at a wind blade plant.

(a) (b)

Figure 4. Automated trailing edge layup; (a) laboratory layup and (b) transfer to wind blade plant production mold

5.2 Literature Review

The shifting theory, or the actual deformation model, is based on a pin-jointed net model, where at each position where the unidirectional and structural tows cross, the joint is assumed to act as a pin, leaving the tows free to rotate. This model was first proposed by Weissenberg from the apparel fabric industry [3] and then adopted by researchers in composite studies[4-6]. In the shifting process at the tow level, the unidirectional tows rotate about the joint while the structural tows shift in the weft direction. This allows for the free movement of the fabric at an angle instead of a curve, as would result if deformed by hand. The shifting method can be seen in Figure 5.

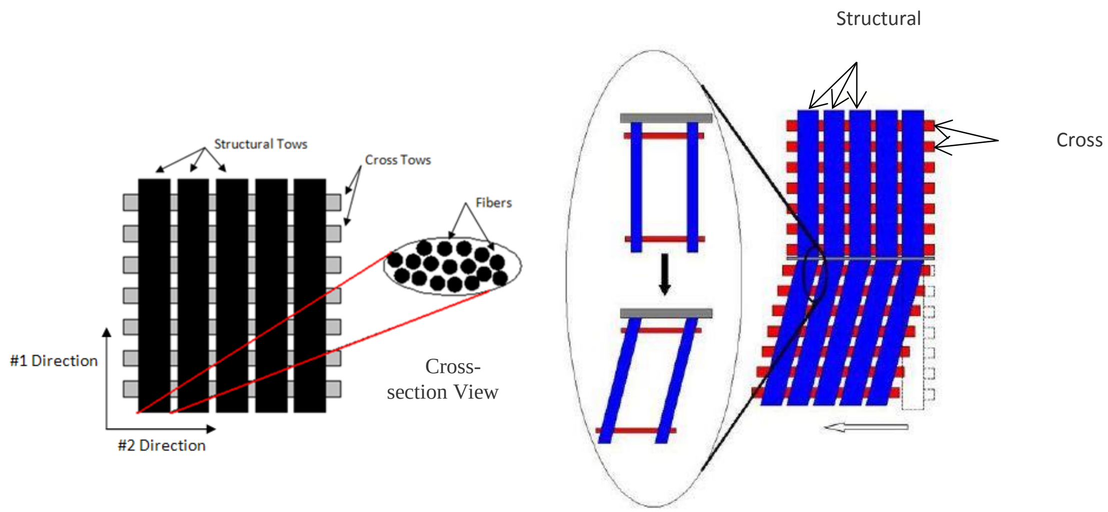

(a) (b)

Figure 5. Shifting; (a) unidirectional fabric structure, and (b) shifting deformation of a panel

Although shifting itself is new, other automation methods involving tow shearing have been studied. In the continuous tow shearing (CTS) method by Kim et al., the fabric was continuously sheared to fit the curvature of a mold [7]. Kim et al. also used microscopic observation to determine fiber orientation and impregnation quality of their sheared carbon fiber tows. [7]

Previous studies verified various aspects of shifting as a new manufacturing method. Magnussen conducted tensile fatigue tests with shifted samples and concluded that the more smooth fabric is shifted, the less effect it will have on material properties[1]. Raghavan conducted compressive fatigue tests and concluded that shifting has negligible effect on properties when the shift degree is less than 10 degrees [8]. The aforementioned two studies investigated the macroscopic properties of cured fiberglass with material test methods. Yet the deformation of the individual fiberglass tows during shifting remained to be observed and understood. The meso-scale testing was necessary because, although the macroscopic effects are what are normally observed when a part performs, the micro- and meso- scale structures are what will cause the macroscopic effects, including possible failures [9].

Meso-scale analysis is not new to composite analysis. Composite fabric is often modeled at the meso-scale level to simulate fabric forming [10] and mechanical properties [11, 12]. Lomov et al. provided a comprehensive summary on literature about meso-scale Finite Element modeling of composites [13]. Some past studies involved experiments that test the meso-scale deformation of composite fabric subjected to stress and deformation [9, 14-16]. Among them, Potluri et al. studied properties of fabric that underwent pure shearing deformation, which was very similar to shifting [17]. In that work, Potlri et al. used a flat-bed scanner to capture the tow geometry after shearing and then measured the tow widths and tow thicknesses after cutting the samples and observed the cross-sections. As shown in Figure 7, cut 1 was along the structural tow direction, and cut 2 was made perpendicular to the unidirectional tow direction [17]. Cut 1 was easier to make but did not expose the true tow width and required trigonometric calculations to find the true width. Cut 2, although significantly more difficult to make accurately, gave access to directly measuring the true tow width instead of being obliged to calculate it, propagating any measurement error.

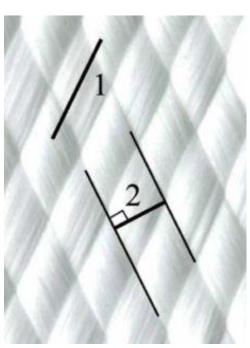

Figure 6. Sample cuts for measuring tow thickness (1) cut parallel to structural tow direction (2) cut perpendicular to unidirectional tow direction [17].

Nelson et al. conducted a series of tests on E-glass fiber glass with common defects found in wind turbine blades manufacturing [18-21]. The work included experiments and modeling on in-plane and out-of-plane waviness. Some of the in-plane waviness flaws identified in their test were very similar to the ones observed by Raghavan [8]. However, the mechanism of how in-plane waviness affects material properties has not been fully understood.

5.3 Experimental Design

A. Experimental Overview

Past studies indicate that the tows in woven fabric generally become thicker/narrower when being sheared [16, 17, 22] and tows were found to be bent at the region close to the clamping mechanism [22]. Because of the similarity between shearing and shifting deformation, this experiment is focused on the change of tow thickness, tow width, space between tows and bend radius after shifting. Fiberglass fabric samples were shifted to different angles to determine how shift angle affects meso-scale deformation, where shift angle is defined as the angle difference of the unidirectional tows before and after shifting (Figure 7). All samples were shifted using a 20% over-shifting technique introduced by Zhu et al. [23] during which fabric was shifted to an angle that is 20% more than the target shift angle and then shifted back to the targeted shift angle. This technique has been shown to reduce shift angle variability among samples. Each sample was divided into six sections for analysis; Section 1 is the straight section that is not shifted, Section 2 and 6 are the clamped sections which are compressed by the shifting clamps, Section 3 and 5 are the bent sections where tows are bent to make tow direction change, and Section 4 is the shifted section where pure shearing occurs. Samples were shifted and scanned by a flat-bed scanner to measure tow width, bend radius and gaps, then mixed with resin and cured to make measurement of the cross-section dimensions possible.

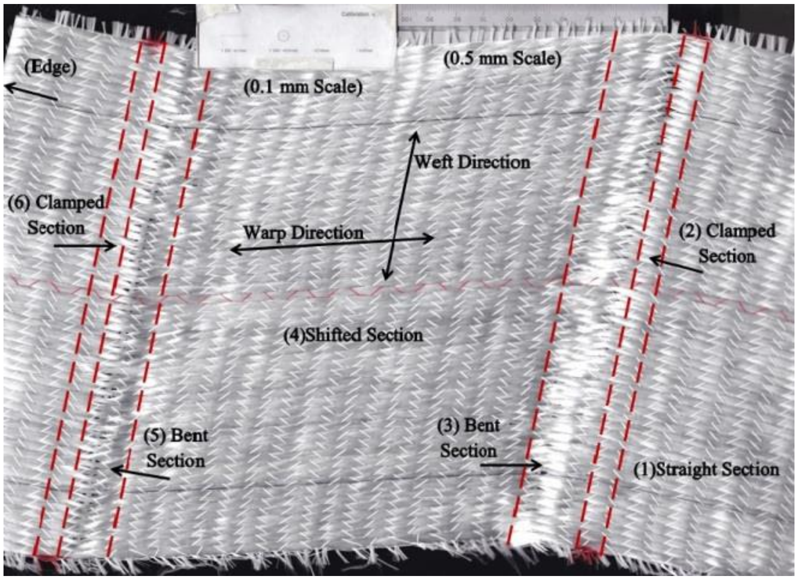

(a)

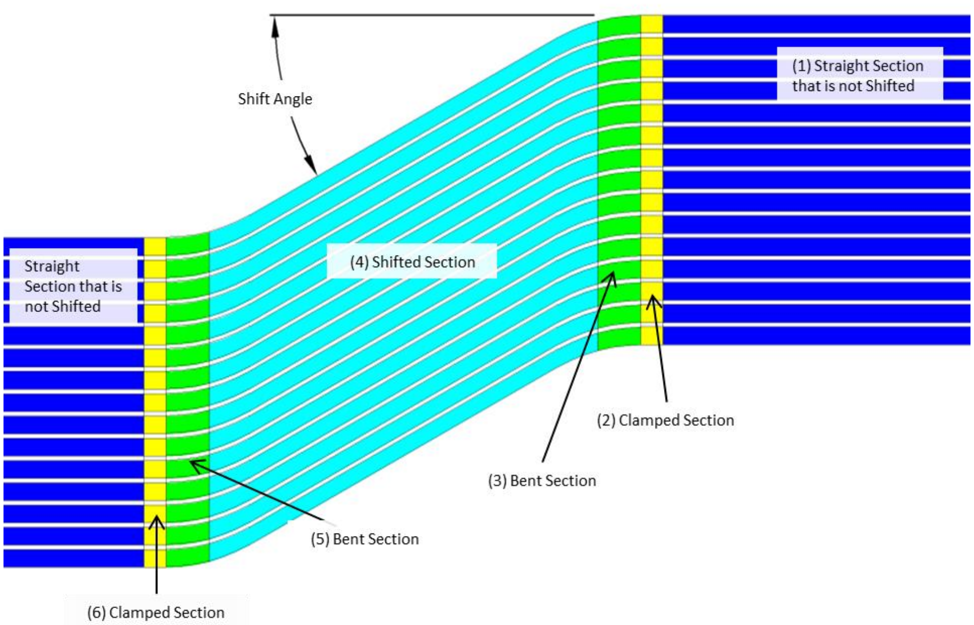

(b)

Figure 7. Sample test sections; (a) shown as image taken by a flatbed scanner and (b) corresponding schematic

B. Sample Creation

Three batches of samples were created using 200 mm wide Saertex 930 g/m^2 unidirectional non-crimped fiberglass (Table 1). Each batch consists of four single-layer fabric samples that were shifted to four different shift angles, 0, 5, 10 and 15 degrees. Note that the 0° samples were processed through the shifting machine, including passing through rollers, but not clamped or shifted. The sequence of sample creation within each batch was randomized. After a sample was generated it was scanned with a Canon LiDE 120 flat-bed scanner immediately to create an image. The image was used to measure tow width, tow bend radius and tow gaps in the ImageJ software package. After scanning, all samples in Batch 2 went through a “tow freezing” process during which fabric was soaked with resin inside a flat mold and cured without being compressed or brushed (analogous to *freezing* the tows in position before measuring and avoid further distortion). All samples in Batch 3 were vacuum infused and cured to imitate industrial manufacturing conditions. After curing, samples in Batch 2 and Batch 3 were cut at various locations perpendicular to the warp direction so that cross-section dimensions of tows can be measured.

Table 1. Samples created for shifting experiment.

Batch # \ Shift Angle \ Sample #	1	2	3	4	Process After Dry Sample is Created and Scanned
1	0°	5°	10°	15°	None
2	0°	5°	10°	15°	Tow Freezing
3	0°	5°	10°	15°	Vacuum Infusing

C. Sample Measurements

Measurements of the fabric tows are mainly focused on three areas: tow width, bent section dimensions and cross-section dimensions. Tow width and bent section dimensions could be measured when the fabric was dry while the cross-section dimensions could only be measured after the fabric was cured with resin.

1) Tow Width

Tow width was measured along the direction perpendicular to the unidirectional tow direction by analyzing pictures of dry samples taken by the flat-bed scanner. The fabric in the straight section and the shifted section were measured for tow width (Figure 7).

2) Bent Tow Dimension and Tow Spacing

The severity of tow bending was measured using the method illustrated in (a)

(b)

Figure 8. A circle was fit to the inner curvature of a bent tow and the radius of the circle was measured to quantify the bend. Some tows were found to split and form gaps within the bent tows in some samples. Hence, the bent sections were also measured for the fraction of gaps. This could an indication of possible resin pockets that could be produced during infusion.

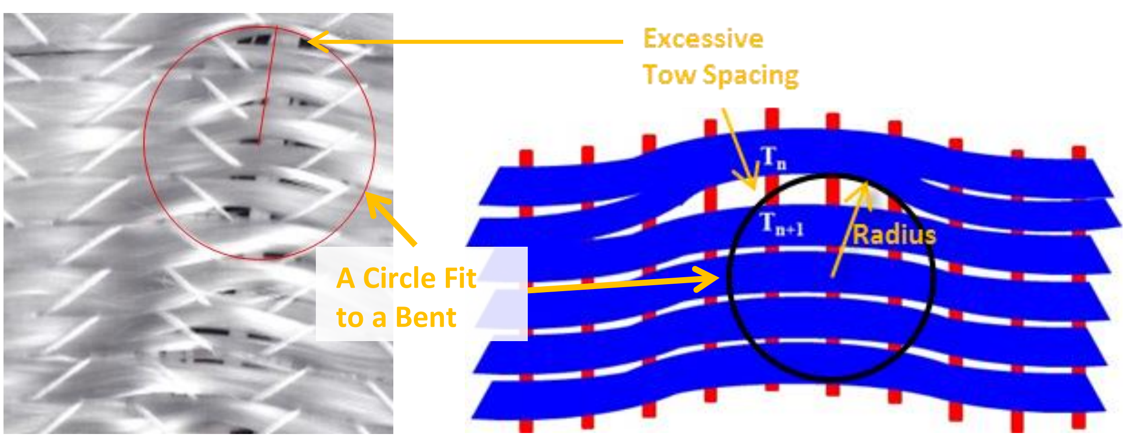

(a) (b)

Figure 8. Measurement of the bent tow radius; (a) shown in an actual photo in Image J and a (b) schematic.

3) Tow Cross Section

Batch 2 and 3 were cut at the straight and shifted section to observe cross-section dimensions after curing. The cuts were made perpendicular to the unidirectional tow direction (Potluri et al. *cut-2* technique) using a waterjet cutter and the cross-section surface was sanded so that the fiber and the resin could be differentiated under a microscope. A microscope was used to photograph the center tow, and the image was processed with ImageJ and Matlab to measure the cross-section dimensions, including tow thickness and cross-section area ((a)

(b)

Figure 9).

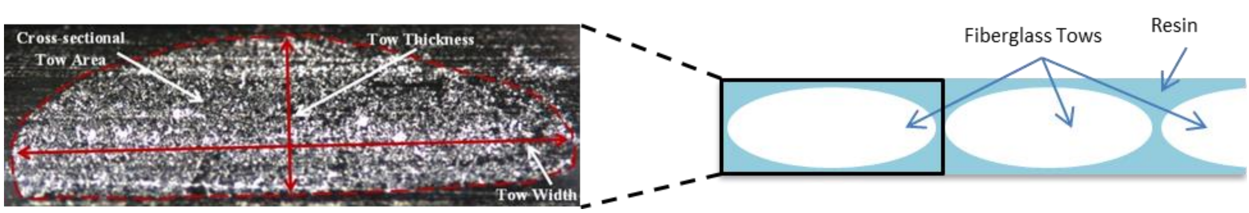

(a) (b)

Figure 9. Tow cross section; (a) Actual microscopic picture and (b) schematic of cross-section view.

5.4 Results and Discussion

A. Tow Width

The ratio between tow width in the shifted section and the straight section within the same sample, referred to as the *Tow Width Reduction Ratio* (*R*), is designated to quantify width reduction after shifting:

$$R = \frac{W_{shifted}}{W_{original}}$$

where $W_{original}$ is the tow width in the straight section representing the tow width before shifting, and $W_{shifted}$ is the tow width in the shifted section after shifting. In the literature there are different theories on tow width change after shearing. Potluri et al. [17] concluded that the tow width in woven fabric did not change when the shear angle was less than 20 degrees. Kim et al. predicted that the theoretical tow width of a shifted prepreg carbon fiber tow should be:

$$W_{shifted} = W_{original} \times \cos(\theta)$$

where θ is the shear angle. Thus,

$$R = \frac{W_{shifted}}{W_{original}} = \cos(\theta)$$

should hold for prepreg carbon fiber tows. The results are shown in Figure 10. The width reduction is significant for the samples shifted to 10 and 15 degrees. The values are lower than cos (θ), indicating that the tow was thinner than Kim's model predicted. It could have been caused by the 20% over-shift but even if a 20% higher angle was used to calculate cos (θ), the predicted R is still significantly higher than the actual values. Also note that, ideally, tow width of the shifted section before shifting instead of the tow width in the straight section should be used for $W_{original}$. However, it was not feasible to do so without deforming the fabric in the current machine configuration.

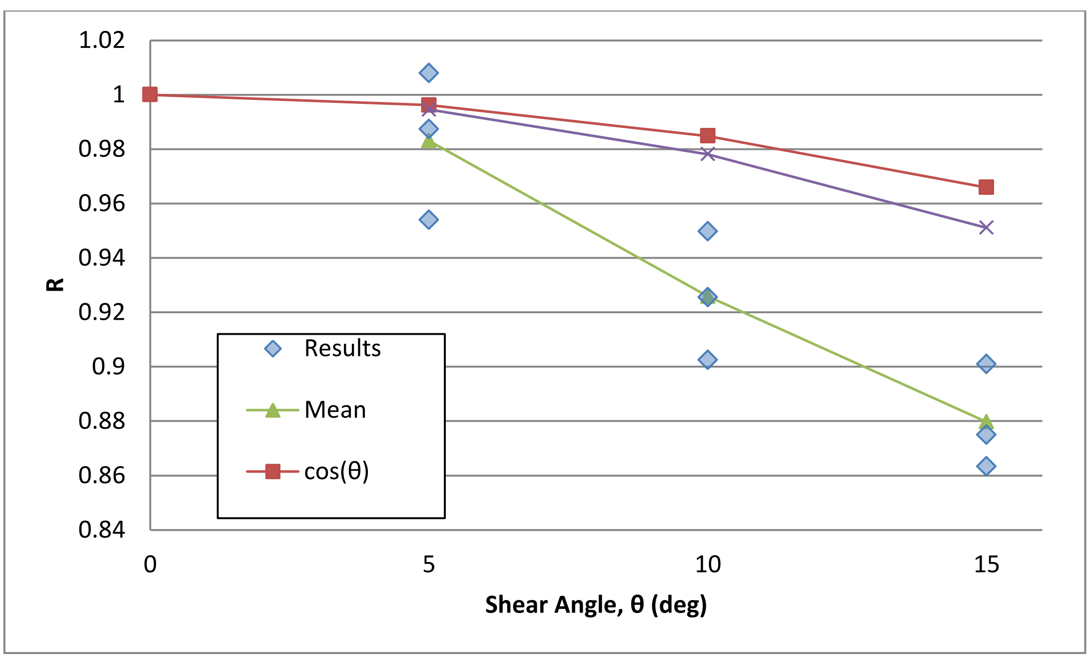

Figure 10. Results for tow width reduction. R = $W_{straight}$ / $W_{shifted}$

B. Bent Tow Radius and Tow Spacing

The radii of curvature for gaps in the bent section varied widely, as shown in Figure 11. The error bars illustrate ±2σ (σ = Standard Deviation). However, no trend can be seen among different shift angles. This indicates that the tows bend similarly for different shift angles, while the arc is longer for higher shift angle to accommodate larger tow direction changes.

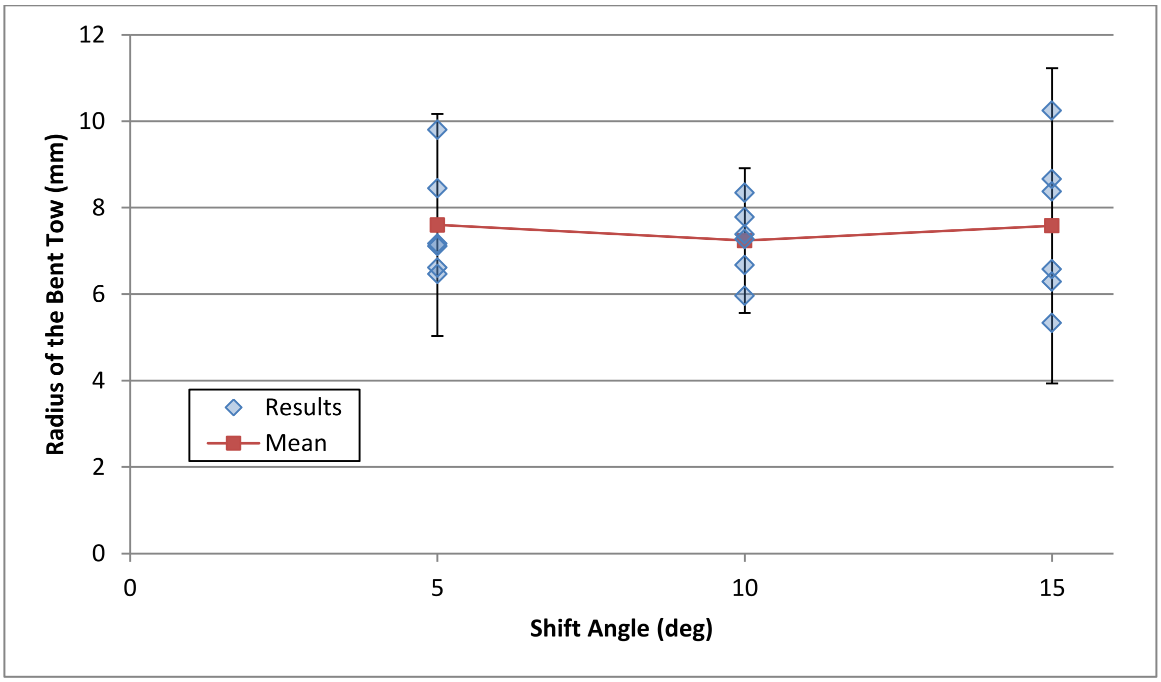

Figure 11. Radius of the Bent Tows. (half error bar width is 2 x standard deviation)

No gap between tows was found in 0° degree samples. Gaps were only found in bent sections of the 5°, 10° and 15° samples. Gaps were quantified and reported as the percentage of space not occupied by fiber (Table 2). High variability was found with the 15° samples. The tow gaps in Section 3, or the bent section next to the shifting clamp, were consistently lower than Section 5, or the bent section next to the spacing clamp. The overall gap percentage can be viewed in Table 2.

Table 2. Gap percentage and stiffness reduction observed from dry samples.

Shift Angle (deg)	Section #	Gap Percentage	Stiffness Reduction
0	N/A	0	0
5	3	0.56%	0.49%
	5	0.47%	0.42%
10	3	2.77%	2.44%
	5	3.07%	2.71%
15	3	6.85%	6.04%
	5	11.42%	10.07%

The gaps may potentially decrease fiber volume fraction in composites which may reduce local stiffness. The stiffness of unidirectional fiberglass can be calculated as:

$$E_c = E_f V_f + E_m V_m$$

where E_f and E_m are the Young's modulus of fiber and matrix, respectively; V_f and V_m are volume fraction of fiber and matrix, respectively. Assuming that the typical E-glass material has the following properties:

$$E_f = 80\ GPa$$

$$E_m = 5\ GPa$$

$$V_f = 0.5$$

$$V_m = 0.5$$

The stiffness with the gaps present can be calculated as:

$$E_c' = E_f V_f' + E_m V_m'$$

$$\begin{cases} V_f' + V_m' = 1 \\ \dfrac{V_m' - V_g}{V_f'} = \dfrac{0.5}{0.5} \end{cases}$$

Where V_g is the gap fraction measured from the experiment.

The stiffness reduction as a fraction of the original Young's modulus can be expressed as:

$$\left(1 - \frac{E_c'}{E_c}\right) \times 100\%$$

The stiffness reduction is listed in Table 2. The stiffness can be reduced by as much as 10 % in the worst case scenario when the fabric is shifted to 15 degrees. However, in the context of wind energy layups the machine is intended for, all the shifts would be within 10 degrees where no more than 2.7 % of stiffness reduction can happen. One way to further mitigate the stiffness reduction is to stagger shift locations across different layers (as they “stack” vertically), by doing so the overall stiffness reduction can be smaller than that for a single layer.

C. Tow Cross-section

The cross-sectional tow area is of interest, in order to see whether the tows are packed more densely after shifting. If tows are packed more densely after shifting, it may decrease permeability and resist resin flow. Figure 12 shows the tow cross-sectional area of the straight section and the shifted section. There is no significant increase or decrease in tow cross-sectional area between the sections in a sample, and no significant difference in the shifted section was found across samples with different shift angles. This indicates that the shifting deformation does not compress or “pack” the tows.

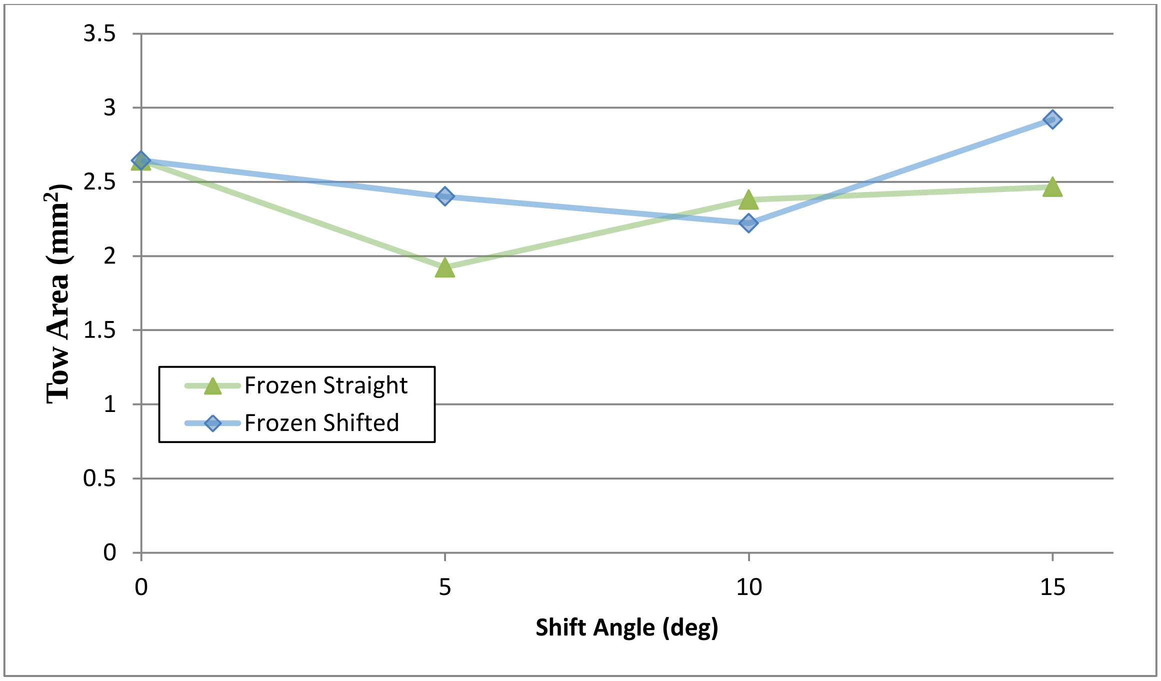

Figure 12. Cross section area of the tows in the shifted sections.

5.6 Conclusion

The meso-scale deformation of fabric due to the shifting mechanism has been studied in this paper. Effects of tow thinning, bending and spacing was observed. The tow widths were observed to reduce during the shifting process. In general, as the shift angle increased, tow width in the shifted section decreased but the cross-section area stayed unchanged, indicating that tows were not packed after shifting. The bent sections saw some effects of an increased shift angle, where the gap percentage increased with the shift angle. The gap radius of curvature did not seem to be influenced by a difference in shift angle.

In closure, the shifting method should provide a suitable method to deform fiberglass fabric in an automated manufacturing process. The work of this paper shows that we can expect limited negative effects in most any case of wind blade manufacturing; much of the analysis showing ill effects were at shifting settings beyond what is necessary for blade geometry.

5.7 References

[1] Magnussen CJ. A fabric deformation methodology for the automation of fiber reinforced polymer composite manufacturing. Ames: Iowa State University; 2011.
[2] Joyce PJ, Moon TJ. Compression strength reduction in composites with in-plane fiber waviness. ASTM special technical publication. 1998;1330:76-96.
[3] Weissenberg K. The use of a trellis model in the mechanics of homogeneous materials. Journal of the Textile Institute Transactions. 1949;40(2):89-110.
[4] Potluri P, Sharma S, Ramgulam R. Comprehensive drape modelling for moulding 3D textile preforms. Composites Part A: Applied Science and Manufacturing. 2001;32(10):1415-24.
[5] Potter K. Beyond the Pin-jointed Net: Maximising the Deformability of Aligned Continuous Fibre Reinforcements. Composites Part A: Applied Science and Manufacturing. 2002;33(5):677-86.
[6] Yu W-R, Harrison P, Long A. Finite element forming simulation for non-crimp fabrics using a non-orthogonal constitutive equation. Composites Part A: Applied Science and Manufacturing. 2005;36(8):1079-93.
[7] Kim BC, Weaver PM, Potter K. Manufacturing characteristics of the continuous tow shearing method for manufacturing of variable angle tow composites. Composites Part A: Applied Science and Manufacturing. 2014;61(0):141-51.
[8] Raghavan LK. Industrial looks at ways of manufacturing defects of fiber reinforced polymer composites: Iowa State University; 2014.
[9] Hamila N, Boisse P. Simulations of textile composite reinforcement draping using a new semi-discrete three node finite element. Composites Part B: Engineering. 2008;39(6):999-1010.
[10] Khan MA, Mabrouki T, Vidal-Sallé E, Boisse P. Numerical and experimental analyses of woven composite reinforcement forming using a hypoelastic behaviour. Application to the double dome benchmark. Journal of Materials Processing Technology. 2010;210(2):378-88.
[11] Edgren F, Mattsson D, Asp LE, Varna J. Formation of damage and its effects on non-crimp fabric reinforced composites loaded in tension. Composites Science and Technology. 2004;64(5):675-92.
[12] Boisse P, Gasser A, Hivet G. Analyses of fabric tensile behaviour: determination of the biaxial tension–strain surfaces and their use in forming simulations. Composites Part A: Applied Science and Manufacturing. 2001;32(10):1395-414.
[13] Lomov SV, Ivanov DS, Verpoest I, Zako M, Kurashiki T, Nakai H, et al. Meso-FE modelling of textile composites: Road map, data flow and algorithms. Composites Science and Technology. 2007;67(9):1870-91.
[14] Potluri P, Parlak I, Ramgulam R, Sagar TV. Analysis of tow deformations in textile preforms subjected to forming forces. Composites Science and Technology. 2006;66(2):297-305.
[15] Boisse P, Buet K, Gasser A, Launay J. Meso/macro-mechanical behaviour of textile reinforcements for thin composites. Composites Science and Technology. 2001;61(3):395-401.
[16] Mohammed U, Lekakou C, Dong L, Bader MG. Shear deformation and micromechanics of woven fabrics. Composites Part A: Applied Science and Manufacturing. 2000;31(4):299-308.
[17] Potluri P, Perez Ciurezu DA, Ramgulam RB. Measurement of meso-scale shear deformations for modelling textile composites. Composites Part A: Applied Science and Manufacturing. 2006;37(2):303-14.
[18] Nelson JW, Riddle TW, Cairns DS. Effects of defects in composite wind turbine blades. Round 2. Sandia National Laboratories; 2012.
[19] Riddle TW, Cairns DS, Nelson JW. Characterization of Manufacturing Defects Common to Composite Wind Turbine Blades: Flaw Characterization. AIAA SDM Conference Denver2011.

[20] Riddle TW, Cairns DS, Nelson JW. Effects of Defects Part A: Stochastic Finite Element Modeling of Wind Turbine Blades with Manufacturing Defects for Reliability Estimation. 54nd AIAA/ASME/ASCE/AHS/ASC Structures, Structural Dynamics and Materials Conference; 2013.
[21] Nelson JW, Cairns DS, Riddle TW, Workman JE. Composite Wind Turbine Blade Effects of Defects: Part B—Progressive Damage Modeling of Fiberglass/Epoxy Laminates with Manufacturing Induced Flaws. 53rd AIAA/ASME/ASCE/AHS/ASC Structures, Structural Dynamics and Materials Conference 20th AIAA/ASME/AHS Adaptive Structures Conference 14th AIAA2012.
[22] McGuinness GB, ÓBrádaigh CM. Characterisation of thermoplastic composite melts in rhombus-shear: the picture-frame experiment. Composites Part A: Applied Science and Manufacturing. 1998;29(1–2):115-32.
[23] Zhu S. An automated fabric layup machine for the manufacturing of fiber reinforced polymer composite. Ames, Iowa2013.

CHAPTER 6 GENERAL CONCLUSION

6.1 Conclusion

This dissertation presented the development of an automated layup system for composite manufacturing. The shifting machine head was designed, implemented and attached to a robotic gantry motion system. The shifting machine demonstrated that shifting is a feasible method to layup fiberglass fabric automatically, with a relatively simple kinematic system. A process planning method was developed in the form of a computer program. The program successfully reads a geometric model of a desired fabric path and generates the corresponding tool path in the form of machine control code. Layup tests showed that the path planning technique could guide the machine to place fabric with relative accuracy to the desired locations. Meso-scale observation and measurement was conducted to investigate the influence of shifting on fabric deformation. The shifting deformation could introduce limited negative effects such as tow gaps when the shift angle is extreme. However, much of these effects were only found when shift setting was beyond what is necessary for the target product; wind blade geometry.

The proposed automated layup system provides a first-of-its kind automated layup solution for broadloom composite fabric with fewer controllable axes and potentially low cost. It could relieve workers from tedious and repetitive work, and the system could save manufacturing time and cost by providing consistent processes and high quality parts.

6.2 Future Work

Future work can be focused on the following areas:

1) Improving accuracy and precision. In wind blade layups, sometimes a gradual change of chordwise distance between layers is needed, which requires very high accuracy. Possible solutions should be investigated to ensure that the process can fulfill stringent manufacturing requirements.

2) Path-planning for multiple layers. Future work can explore the path-planning techniques for multiple layers. The distribution of shift locations and the length of shifts can be optimized with the consideration of multiple layers. For example, shift locations of multiple layers can be distributed wisely to cover as much area as possible for highly curved areas of the mold.

3) Mitigating material degradation. Although the negative effects caused by the shifting deformation were found to be small for wind energy applications, these effects can possibly be mitigated by better process planning. For example, to mitigate the stiffness reduction caused by the tow gaps, shifting location can be staggered across different layers instead of stacking on top of each other vertically. Hence, the overall stiffness reduction for a multiple-layer construct can be smaller than that for a single layer.

3) Material analysis on a full scale. The material testing conducted in this dissertation consisted of tensile coupon testing and meso-scale measurements on shifted fabric samples. Full scale material testing on an actual component was not conducted because of the constraints in the lab setup. It would be desirable to conduct material tests on a trailing edge component made with the fabric shifting system and compare the results with a part made from the traditional production process.

4) Cost effectiveness analysis. Wind blade manufacturing is sensitive to cost and capital investment. A relatively simple kinematic system was designed for the fabric shifting head to keep the cost low. Hence the most costly component for the current system is the robotic gantry. Possibility of replacing the gantry with a novel motion system with lower cost and similar precision and accuracy should be analyzed. Such a motion system could be a custom built rail-guided cart or an autonomous industrial vehicle that can move across the shop floor.